FOR FURTHER TRAN

(12)

CR 78.012

CIVIL ENGINEERING LABORATORY
Naval Construction Battalion Center
Port Hueneme, California

Sponsored by
NAVAL FACILITIES ENGINEERING COMMAND

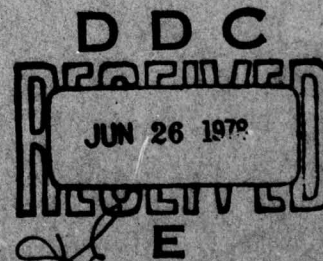MATERIALS STUDY FOR HIGH
PRESSURE SEAWATER HYDRAULIC
TOOL MOTORS

April 1978

D D C
JUN 26 1978
E

An Investigation Conducted by

MECHANICAL TECHNOLOGY INC.
Latham, New York

78 06 12 091

REPORT DOCUMENTATION PAGE		READ INSTRUCTIONS BEFORE COMPLETING FORM
1. REPORT NUMBER CR-78.012	2. GOVT ACCESSION NO. CEL	3. RECIPIENT'S CATALOG NUMBER
4. TITLE (and Subtitle) Materials Study For High Pressure Sea Water Hydraulic Tool Motors		5. TYPE OF REPORT & PERIOD COVERED Final Report April - Dec 78 6. PERFORMING ORG. REPORT NUMBER MTI-78TR45
7. AUTHOR(s) Bharat Bhushan and Stanley Gray		8. CONTRACT OR GRANT NUMBER(s) N68305-77-C-0001
9. PERFORMING ORGANIZATION NAME AND ADDRESS Mechanical Technology Inc. 968 Albany-Shaker Road Latham, New York 12110		10. PROGRAM ELEMENT, PROJECT, TASK AREA & WORK UNIT NUMBERS 62759N; YF52.556.091.01.309
11. CONTROLLING OFFICE NAME AND ADDRESS Naval Construction Batallion Center Port Hueneme, California		12. REPORT DATE February 15, 1978 13. NUMBER OF PAGES 165
14. MONITORING AGENCY NAME & ADDRESS(if different from Controlling Office) Apr 78		15. SECURITY CLASS. (of this report) Unclassified 15a. DECLASSIFICATION/DOWNGRADING SCHEDULE
16. DISTRIBUTION STATEMENT (of this Report) Approved for public release; distribution unlimited YF52.556 YF52.556.097		169 p.

17. DISTRIBUTION STATEMENT (of the abstract entered in Block 20, if different from Report)

DDC
RECEIVED
JUN 26 1978
E

18. SUPPLEMENTARY NOTES

19. KEY WORDS (Continue on reverse side if necessary and identify by block number)

Hydraulic Motor	Vane Motor
Piston Motor	Sea Water Lubrication
Gear Motor	Friction and Wear

20. ABSTRACT (Continue on reverse side if necessary and identify by block number)

The objective of the program was to conduct a comprehensive materials study for a small, compact, positive displacement hydraulic motor which will use pressurized sea water as the working fluid. Gear, vane and piston-type motors were selected for the study. The design analysis of the critical components of each motor type were conducted using a baseline motor size of 10 gpm at 1000 psi and 5.8 input horsepower in order to establish the loading and speed requirements. Based on material requirements, an extensive literature search was conducted of published test data on materials, data

78 06 12 091224550

relevant to sea water lubricated conditions. In the event that test data on materials was not available, tests were conducted to obtain friction, wear and corrosion data under simulated conditions. Two test rigs were prepared for the studies, one a continuous sliding tester capable of up to 2000 psi at 1500 fpm, and the other a reciprocating tester capable of up to 1500 psi and 250 fpm average speed. The material combinations tested included plastic-metal, metal-metal and nonmetal-metal categories. Submersion tests in sea water were conducted to study corrosion resistance of selected metals and metal couples. Particularly successful combinations in the material testings were: Torlon 4301 (Polyamide-imide with fillers) versus Inco 625, and High purity Alumina Versus Plasma sprayed Tungsten Carbide.

In the continuing design analysis of the motor types, techniques for balancing the internal loads to reduce the contact requirements, and techniques for self-adjustments for wear rate were studied and developed. In the overall assessment of suitability to sea water operation, top ranking was given to the double entry vane motor, this followed by the double row axial piston multi-lobe cam design. The materials evaluated in the study were particularly well matched to the vane motor.

Future work recommendations for continuing sea water motor development included: building and developing a double entry vane motor, an experimental and analytical study of rolling and rolling-plus-sliding contact conditions under sea water lubrication conditions, and further studies of a more basic nature of the lubrication improvements possible with very small quantities of soluble additions and those from reactive motor materials.

TABLE OF CONTENTS

TABLE OF CONTENTS (CONT'D)

LIST OF FIGURES

LIST OF FIGURES (CONT'D)

LIST OF FIGURES (CONT'D)

LIST OF TABLES

ABSTRACT

The objective of the program was to conduct a comprehensive materials study
for a small, compact, positive displacement hydraulic motor which will use
pressurized sea water as the working fluid. Gear, vane and piston-type
motors were selected for the study. The design analyses of the critical
components of each motor type were conducted using a baseline motor size of
10 gpm at 1000 psi and 5.8 input horsepower in order to establish the load-
ing and speed requirements. Based on material requirements, an extensive
literature search was conducted of published test data on materials, data
relevant to sea water lubricated conditions. In the event that test data
on materials was not available, tests were conducted to obtain friction,
wear and corrosion data under simulated conditions. Two test rigs were pre-
pared for the studies, one a continuous sliding tester capable of up to 2000
psi at 1500 fpm, and the other a reciprocating tester capable of up to 1500
psi and 250 fpm average speed. The material combinations tested included
plastic-metal, metal-metal and nonmetal-metal categories. Submersion tests
in sea water were conducted to study corrosion resistance of selected metals
and metal couples. Particularly successful combinations in the material test-
ings were: Torlon 4301 (Polyamide-imide with fillers) versus Inco 625, and High
purity Alumina Versus Plasma sprayed Tungsten Carbide.

In the continuing design analysis of the motor types, techniques for balancing
the internal loads to reduce the contact requirements, and techniques for self-
adjustments for wear rate were studied and developed. In the overall assessment
of suitability to sea water operation, top ranking was given to the double entry
vane motor, this followed by the double row axial piston multi-lobe cam design.
The materials evaluated in the study were particularly well matched to the vane
motor.

Future work recommendations for continuing sea water motor development included:
building and developing a double entry vane motor, an experimental and analytical
study of rolling and rolling-plus-sliding contact conditions under sea water
lubrication conditions, and further studies of a more basic nature of the lub-
rication improvements possible with very small quantities of soluble additions and
those from reactive motor materials.

FOREWORD

The research described herein, which was conducted by Mechanical Technology Incorporated under CEL Contract N68305-77-C-0001, was performed under the project management of Mr. Stanley A. Black, Research Mechanical Engineer, Civil Engineering Laboratory, Naval Construction Batallion Center. The authors wish to thank Mr. Rolf Ziegler for some of the design layout studies and Messrs. J. Wilson and E. Beach for their help in the experiments.

1.0 INTRODUCTION

1.1 Background

Most of the power hand tools used by Navy divers are operated by oil hydraulic motors. Dual hoses supply the hydraulic oil from the power supply located at the sea surface. The use of oil hydraulic systems has many disadvantages, some of which include:

- Leakage of working fluid contaminates the environment.

- Leakage of sea water can damage the internal parts of the motor.

- From the diver's standpoint, the need for two hoses burdens tool handling.

A hydraulic motor designed to operate on filtered sea water delivered under pressure from the sea surface and discharged into the sea at the tool will eliminate these disadvantages. A limited effort has been put into developing such a motor in the last decade (for a summary of past efforts to develop sea water motors see Black [1]). Since sea water is corrosive in nature and has low viscosity and poor lubricity, the selection of materials which will have the desired corrosion, friction, and wear properties becomes a major challenge. Based on design studies, the positive displacement-type of motors have been recommended as a result of their high output-to-weight ratio (i.e., compactness and other factors).

1.2 Program Objectives

The broad objective of the development effort of this program was to study sea water activated positive displacement-type hydraulic motors for delivery of power levels of 5-10 hp at speeds in the range of 1000 to 15,000 rpm, using sea water at pressures of 1000 psi or greater. The desired physical and operational characteristics are reviewed in Table 1.1. The specific objective of this program was to recommend one or more motor designs primarily based on the availability of materials capable of working in the sea water environment, and to provide material performance data for selected materials when it is not already available.

1.3 Program Approach

The program was divided into three distinct parts. These include:

1.3.1 Sea Water Hydraulic Motor Material Requirements

The objective of this program segment was to examine and analyze candidate motor design approaches, to determine the critical areas from the standpoint of material durability and the maintenance of motor efficiency, and to establish the specific material requirements that must be met.

1.3.2 Material Properties

For those materials about which wear and/or corrosion data was needed as determined in Section 1.3.1, experimental measurements under conditions of load, surface velocity, temperature, and reciprocation were carried out as close as practicable to the anticipated motor conditions.

Table 1.1

DESIRED PHYSICAL AND OPERATION CHARACTERISTICS FOR A SEA WATER HYDRAULIC TOOL MOTOR

Parameter	Value	Comments
Power Output (Hp)	3 Minimum	Adaptable to higher power development.
Speed - Optional (rpm)	1000 - 15000	Selection depends on developmental difficulty.
Operational Efficiency (%)	70	High to maintain overall system efficiencies.
Minimum Operational Pressure (psi)	1000	Or higher desirable to minimize system flow rates.
Maximum Flow Rate (gpm)	7 - 10	Low values desirable to minimize hose diameter and maintain high transmission line efficiencies.
In Water Weight (lbs)	5 - 15	Without using buoyancy materials.
Volume (cu. in.)	10 - 50	Smaller desirable for ease of diver handling.
Maximum Length (in.)	3 - 6	Smallest desirable to allow diver easy access to work surface.
Maximum Width (in.)	2 - 4	Smallest desirable to prevent restriction of diver visual field.

1.3.3 Motor Concepts and Recommendations

Based on the motor analyses and the material properties from Sections 1.3.1 and 1.3.2, one or more motor concepts for further development were recommended.

The recommendations shall include possible concepts for load sharing, load reduction methods where these may relieve excessive material bearing loads, and major features and specifications for the motor concept(s) as a guide to future motor development.

2.0 DETERMINATION OF SEA WATER MOTOR MATERIAL REQUIREMENTS

2.1 Introduction and Discussion of Evaluation Techniques

Potentially, there are a large number of positive displacement, hydraulic motors and an even greater number of variations which could conceivably be considered for powering underwater tools.

In this study, three of the most promising types of motors: gear, vane, and piston, together with some limited variations within the basic types, were selected for a more detailed design analysis of critical elements. From this analysis, motor material requirements have been established.

The selected motors and design variations for the study are listed in Table 2.1.

TABLE 2.1

SELECTED MOTORS AND VARIATIONS

Motor Types

Gear	Radial Rotating Vane	Axial Multi-Piston
• External mesh Internal mesh	• Single entry	• Single piston row with flat cam plate
• Series or Multiple Contact	• Double entry	• Double opposed piston rows with three lobe cams
• Special Tooth Profiles		

In order to reduce the number and range of physical and operational characteristics for the motors given in Table 2.1 to a handleable quantity, some simplifications became necessary. These simplifications, which are discussed below, give representative motor requirements and permit comparisons to be made between motor types.

A constant inlet fluid horsepower of 5.8 has been used, derived from a hypothetical performance of 10 gpm inlet flow (Q) at 1000 psi (P). Within the fixed constant horsepower limit, variations of inlet pressure, inlet flow, and motor speed have been studied.

Since it is not practical at this point to estimate the variations of mechanical and volumetric efficiencies with motor types, pressure, flow, speed, etc., efficiency loss influences have not been included in the analysis.

On this basis, motors have been sized as follows:

- Fluid $HP_{in} = \dfrac{P \times Q}{1714}$

  $= \dfrac{1000 \times 10}{1714} = 5.8\ HP$

Range of variations included in the study are:

- Maximum Inlet Pressure, psi: 1000 - 1500

- Maximum Inlet Flow, gpm: 6.64 - 10

- Maximum Speed Range, rpm: 625 - 4825

The detailed analysis of the motor types has been divided into three major sections covering gear, vane, and piston motors. Motors have been sized for the constant input horsepower with a view to achieving the most compact packages consistent with realistic motor speeds and flow velocities. A design life of 200 hours minimum has been assumed. The scope of the work did not permit optimization of designs.

In hydraulic machinery, the loaded and relatively moving surfaces are generally operating in sliding and are ideally separated by a thick lubricating fluid film. The load support generated in the fluid film may be from hydrostatic (external pressure sources), hydrodynamic (self-generated from relative sliding), squeeze film actions (rapid approach of two parallel surfaces), or quite commonly some combination of these actions.

Because of the low viscosity of the sea water and the relatively high loading used in motor designs in order to achieve compact tools, very thin fluid films may exist which put the operating regime into the "mixed lubrication" regime

on the familiar $\frac{ZN}{P}$ versus friction plot. Even worse the "boundary lubrication"

regime may be experienced, where the self-lubricating or anti-galling properties of mating materials became extremely important. The benefits of squeeze film action are probably quite small because of the low water viscosity and component configurations and motions, but it is necessary to determine the potential significance of hydrodynamic support under representative motor operating conditions.

Taking, as an example, a well designed sea water lubricated journal bearing of 1 inch diameter, operating with a load of 800 psi on the projected bearing area at 5,000 rpm (such as might occur in a gear type motor), it can be shown that the minimum film thickness in the bearing which supports the load hydrodynamically will be less than 0.0001 inch. This illustrates that, in order to achieve any meaningful hydrodynamic support, extremely accurate components and surfaces are necessary. Hydrostatic support and balancing of internal loading, using the input pressure, offers the most promising method of achieving greater film thickness, albeit at the expense of additional fluid flow.

From the Chapter 2 analyses, representative velocities, pressures, and PV levels have been determined which can be related to potential material properties. The chapter concludes with a table summarizing the more pertinent material performance requirements for all three motor types.

2.2 Gear Motor Material Requirements

The gear motor is attractive because of the apparent simplicity, small number of parts, and potentially low weight/horsepower ratio as indicated in Figure 2.1 (Reference 2), which gives a comparison of oil-lubricated motors.

Parameter	Gear-on Gear	Gear-in-Gear	Differential Gear	Crescent Gear	Radial Vane*	Rotary Vane	Radial Piston (Rotary Barrel)	Radial Piston (Fixed Cylinder)	Axial Piston
					Properties of Hydraulic Motors				
Maximum Continuous Pressure (psi)	3,000	2,000	1,500	500	2,500	2,000	3,000	5,000	2,500–5,000
Displacement (cu. in./rev)	20	5	15	–	12	10	98	2,310	44
Maximum Torque (lb-in.)	6,000	1,500	3,700	–	4,000	3,200	46,000	1,100,000	17,500
Starting Torque (% of theoretical)	70	70	68	60	70	99	88	97	72
Running Torque (% of theoretical)	90	87	85	95	90	95	95	97	93
Continuous Speed Range (rpm)	100–3,000	100–5,000	12–1,000	200–5,000	80–4,000	5–1,000	1–2,000	0–300	50–4,500
Maximum Continuous Power (HP)	200	100	32	–	140	70	250	300	413
Leakage (% of max theoretical displ.)	8	10	15	20	2.5	3	3	3.5	2.5
Weight-to-Power Ratio (lb/HP)	0.2	0.2	1.5	0.8	0.3	1.1	2	2	0.7

* Data given for 4-ramp models.

Figure 2.1. General Comparison of Wide Range of Oil Lubricated Motors (Ref. 2)

Both external and internal mesh designs are of interest: the internal because it offers the possibility of reduced gear contact stresses from low meshing speeds and conforming tooth profiles at the expense of potentially greater internal leakage.

External gear pumps have been estensively used on aircraft gas turbines for pumping low viscosity kerosene and gasoline at high pressures. The usual motor and pump designs of both external mesh (Figure 2.2) and internal mesh (Figure 2.3) types have single entry and exit ports. They are sometimes arranged in series to give a lower loading level per stage at the expense of greater bulk. Similarly, in an external gear motor, a central power output "sun" gear with two or more fixed planet gears might be feasible to reduce gear contact stresses and some bearing loading at the expense of bulk, complication, and greater internal leakage. One internal gear pump design (Reference 3) claims the use of an improved tooth profile which inherently generates greater hydrodynamic support and reduces the tooth contact stresses. Figure 2.3 is taken from this reference.

Some of the anticipated critical design factors in gear motors, from a sea water materials/lubrication point of view, are as follows:

- Contact stresses during the gear mesh

- Bearing loads

- Gear deflections in housing

- Gear fabrication difficulties for special materials

- Sensitivity to contamination wear

- Motor starting without pressure balancing

2.2.1 Study of Gear Teeth Stresses

In determining the gear contact stresses, an external gear configuration was selected based on some kerosene lubricated gear pump experience; Figure 2.4 illustrates a basic external gear motor arrangement for a design sized to handle 10 gpm flow at 1000 psi supply pressure at 2500 rpm. The same basic gear design was used to analyze an internal gear motor design of the general configuration illustrated in Figure 2.4. The designs were analyzed using MTI computer codes for both the internal and external mesh arrangement, and both steel and plastic gears were considered. Assumptions in the study included:

Tooth Profile:	Involute	
Number of Teeth:	10 x 10 external	10 x 20 internal
Operating Pressure Angle, degrees:	28-1/2 external	20 internal
Contact Ratio:	1.227 external	1.627 internal
Diametral Pitch:	8.46 (3 module)	
Modulus of Elasticity, psi:	30×10^6 steel 0.2×10^6 plastic	

'O' RING OIL SEALS

LOW PRESSURE DUCT

PRESSURISED BEARING

LOW PRESSURE AREA

HIGH PRESSURE AREA

HIGH PRESSURE DUCT

HIGH PRESSURE AREA

INLET

OUTLET

TYPICAL BEARING
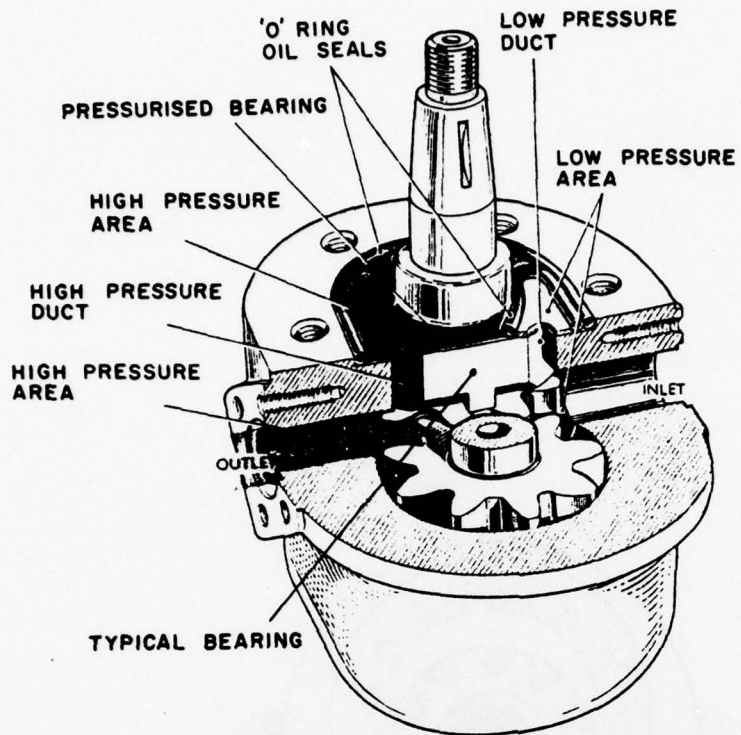
The principle of hydraulically loading the bearings against the gear side faces is shown.

BB

AA

A

B

BB

AA
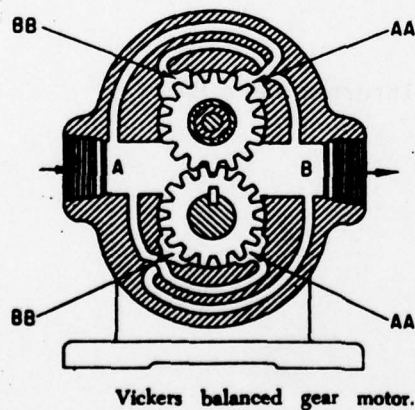
The concept for hydraulically balancing gear and bearing loads is shown.

Vickers balanced gear motor.

Figure 2.2 Gear Pumps and Motor

MECHANICAL TECHNOLOGY INCORPORATED
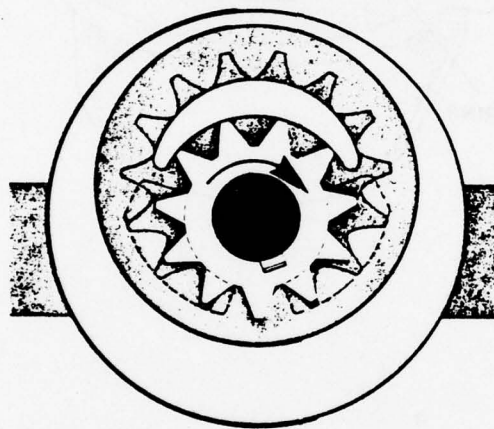
Figure 2.3   Internal Gear Motor

PRESSURE LOADED SIDE PLATES

PRESSURE BALANCE CONCEPT

FLUID PRESSURE

NARROW BEARIN SUPPORT TO PROVIDE SOME SELF ALIGNMEN

JOURNAL BEARING

2500 RPM IO GPM 1000 PSI

A A

PRESSURE BALANCE CONCEPT

HP

LP

SECTION A-A
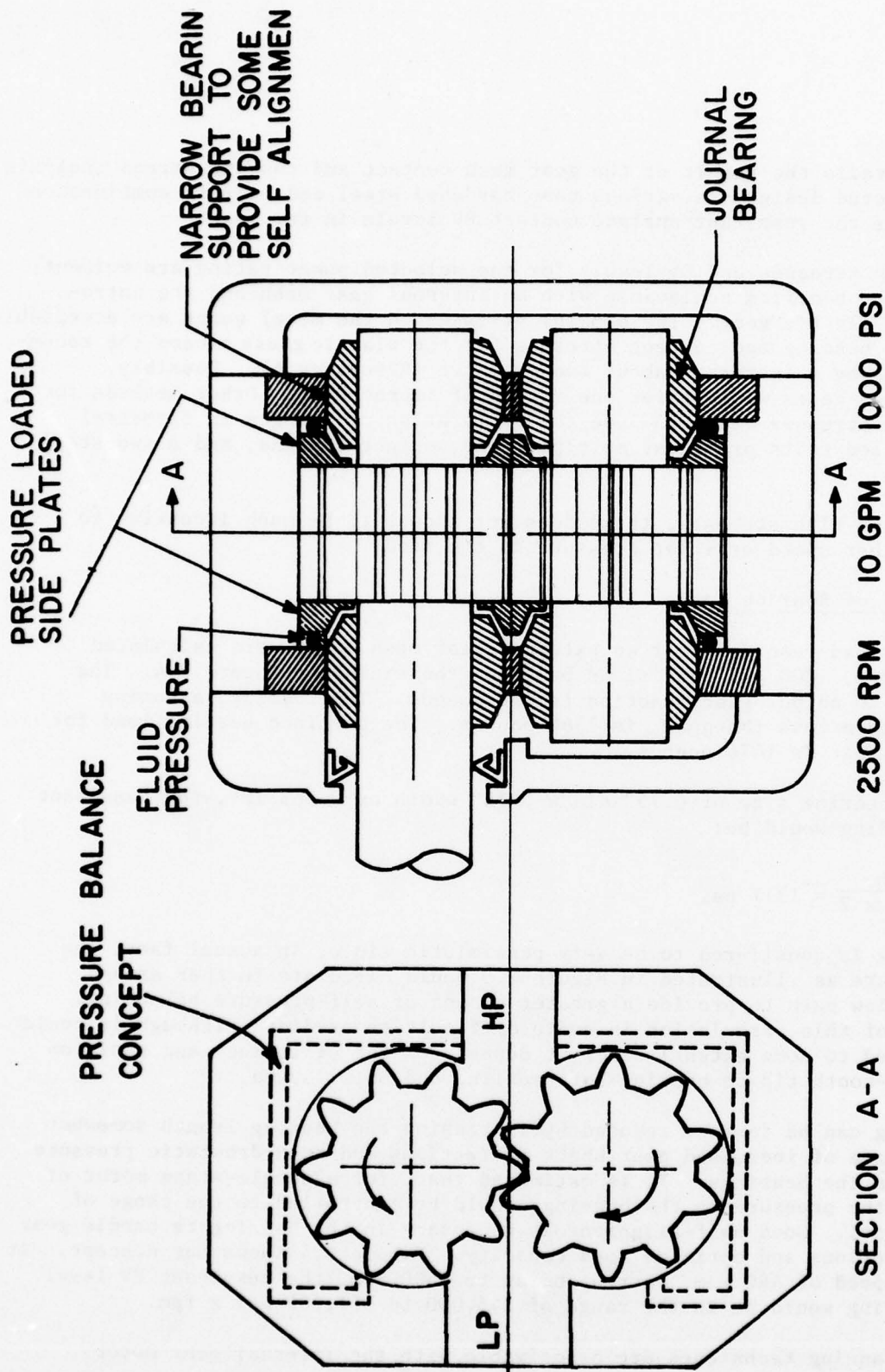
Fig. 2.4 Gear Motor Concept - Sea Water Tool

Table 2.2 details the result of the gear mesh contact and bending stress analysis for the selected designs in various case hardened steel and plastic combinations. Also given is the resultant surface contact PV levels in the mesh.

The very high stresses and PV levels for the selected power rating are evident, as well as the benefits achievable with an internal gear mesh and the introduction of a plastic gear. The bending stresses on the metal gears are acceptable, but both the bending and contact stresses for the plastic gears exceed the recommended levels by a factor of about two or three (Reference 4). Possibly, plastic coated gears would offer one method of improvement. Other methods for reducing the stresses could include the exploration of changes in diametral pitch, modified tooth profiles, multiple gear contact designs, and a two-stage motor.

Because of the high stresses, there does not appear to be much incentive to increase either speed or inlet pressure in the study.

2.2.2 Study of Bearing Loads

The bearing load reactions for an external gear mesh motor were calculated for the 10 gpm, 1000 psi conditions based on the sizing of Figure 2.4. The loading due to output gear reaction is 116 pounds. The loading, assuming 1000 psi acts across the gear, is 1360 pounds. The combined bearing load for the "idler" gear is 1476 pounds.

Based on a bearing size of 0.75" dia x 0.75" width or 0.563 in^2, the resultant bearing loading would be:

$$\frac{1476}{0.563 \times 2} = 1317 \text{ psi}$$

This loading is considered to be very pessimistic since, in actual fact, the inlet pressure as illustrated in Figure 2.5 would circulate further around the motor flow path to provide a greater amount of self-pressure balancing. The extent of this circulation is quite difficult to predict (although it could be controlled to some extent) since it depends on the efficiency and position of the gear-tooth tip to housing-bore sealing and motor speed.

This loading can be further reduced by increasing the bearing length somewhat at the expense of increased gear shaft deflections and by hydrostatic pressure balancing in the bearings. It is estimated that, for a single-stage motor of this type, the pressure in the bearings could be controlled to the range of 500 to 750 psi. Good self-alignment is necessary in the bearing to handle gear shaft deflections and optimize load capacity. Figure 2.4 shows one concept. At a surface speed of 490 fpm, corresponding to 2500 rpm, the resultant PV level in the bearing would be in the range of 245,000 to 367,000 psi x fpm.

Similar balancing techniques are conceivable with the internal gear motor.

Stiffness of the bearing, both in the fluid film and construction materials, and bearing clearance must be in line with the positioning accuracy required for the gears in the housing. If plastic bearings appear attractive, then they would probably have to be in the form of thin liners supported in metal sleeves.

TABLE 2.2

ANALYSIS OF GEAR MOTOR TOOTH STRESSES EXTERNAL AND INTERNAL MESH

Combination Pinion/Gear	Pinion		Gear		Pitch Line Velocity fpm	Peak Sliding Velocity fpm	Peak Surface PV at Contact psi x fpm
	Surface Stress lb/in.²	Tooth Bending Stress lb/in²	Surface Stress lb/in.²	Tooth Bending Stress lb/in²			
External Mesh							
Steel/Steel	102,500	4800	102,500	4800	827	555	56,890,000
Steel/Plastic	11,800	4800	11,800	4800	827	555	6,550,000
Plastic/Plastic	8,370	4800	8,370	4800	827	555	4,650,000
*Plastic/Plastic	10,250	7190	10,250	7190	827	555	5,690,000
Internal Mesh							
Steel/Steel	62,240	5100	62,240	5100	773	206	12,800,000
Steel/Plastic	7,160	5100	7,160	5100	773	206	1,475,000

Input Speed: 2500 rpm
Input Pressure: 1000 psi

External Mesh: 10 teeth x 10 teeth
Internal Mesh: 10 teeth x 20 teeth

* Input Pressure: 1500 psi

HIGH PRESSURE
INLET

DISCHARGE

POSSIBLE PRESSURE
PROFILES AROUND
MOTOR, DEPENDING
ON SEALING EFFICIENCY
AND SPEED
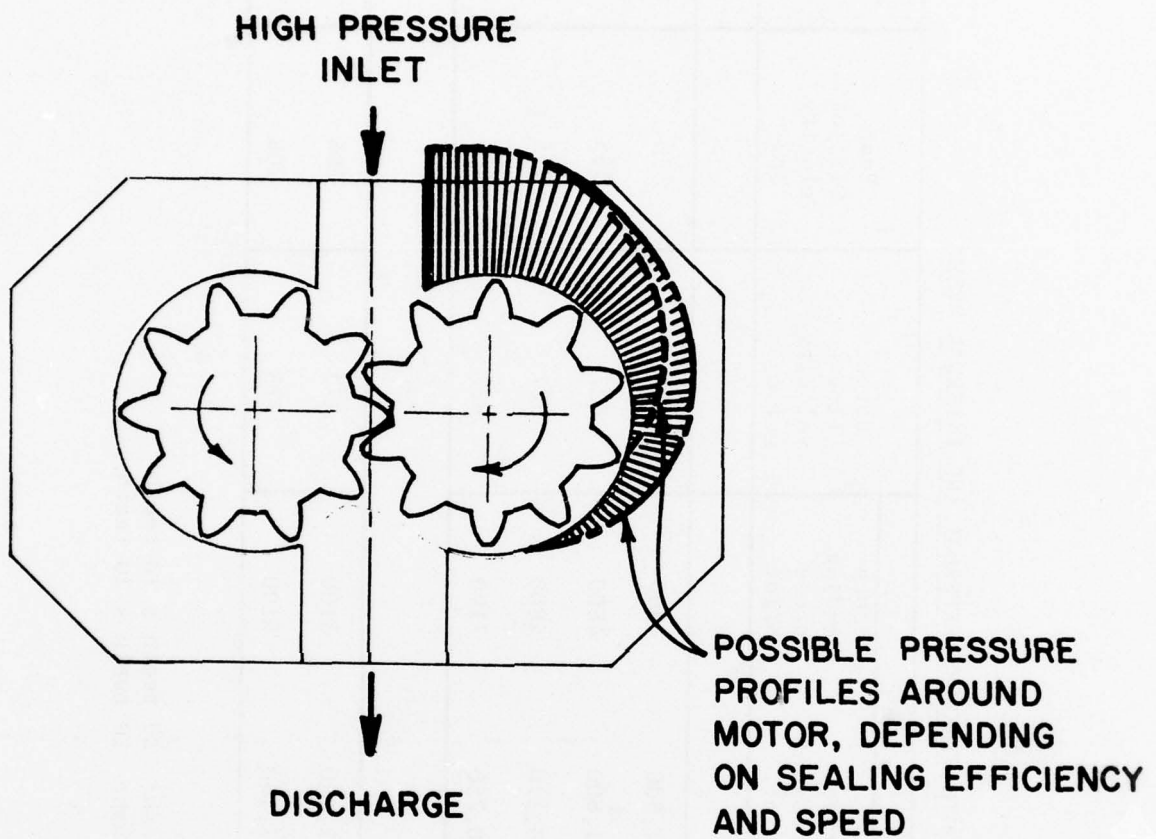
Figure 2.5   Estimated Pressure Profiles Around Gear Motor
Giving Some Bearing and Internal Load Balancing
(Based on data from gear pump tests)

2.2.3 Gear Side Face Loading

As illustrated in Figures 2.2 (upper illustration) and 2.4, the concept of floating and pressure loaded side walls or faces have been selected in order to control the gear sideface leakage, in Figure 2.2 (upper) each journal bearing is independent and pressure loaded against the gear side faces while in Figure 2.4 two floating side plates are used. Theoretically, by carefully engineering the pressure balance area behind the floating side walls to match the pressure gradient through the flow path, the unbalance loading between the gear ends and the side walls can be very nominal, consequently with good mechanical design and material compatibility this should not be one of the most critical design areas.

2.2.4 Gear Deflection in Housing

Assuming that the gear is integral with a high strength shaft of a material such as steel, and that the equivalent journal diameter stiffness is maintained between bearings, then the center deflection at these inlet pressure conditions would not present any problems. If composite gear shaft construction is used, possibly with plastics or ceramic type materials, then careful checking of both stresses and deflections would be required.

2.3 Vane Motor Materials Requirements

The radial vane motor is attractive because of: the relatively small number of simple parts and ease of machining; its acceptable weight/horsepower ratio with multiple inlets (Figure 2.6); balanced bearing loads and low operating speed with multiple inlets; and possible self-compensation of vane tip wear and ease ease of vane replacement.

Some of the anticipated critical factors in vane motors, from a material/ lubrication point of view, are as follows:

- Vane tip wear

- Vane side loading in rotor

- Sealing around vanes and rotor

Because of the significant advantages of a double-inlet vane motor over a single-inlet, only the double-inlet design has been studied. Figure 2.6 shows the basic design concept.

2.3.1 Study of Vane Tip Operation

The study is based on three combinations of supply pressure, system flow, and speed, all of equivalent input power as indicated in Table 2.3 and shown on Figure 2.7. Figure 2.7 also shows the relative size of the three concepts.

A detailed examination was made of the two extreme cases, A and C, assuming the following vane and vane track material candidates:

Vane		Vane Track
Plastic	vs.	Inconel
Inconel with Tungsten Carbide Surface	vs.	Inconel Coated with Aluminum Oxide or Aluminum Oxide

2-11

TYPICAL
PRESSURE FEED
(OR BLEED) TO
BOTTOM OF VANE

INLET PORT

SECTION A-A

2500 RPM   10 GPM   1000 PSI

HYDRAULIC SIDE
LOAD BALANCING
FROM PRESSURE
HERE

INLET PORT

A

A
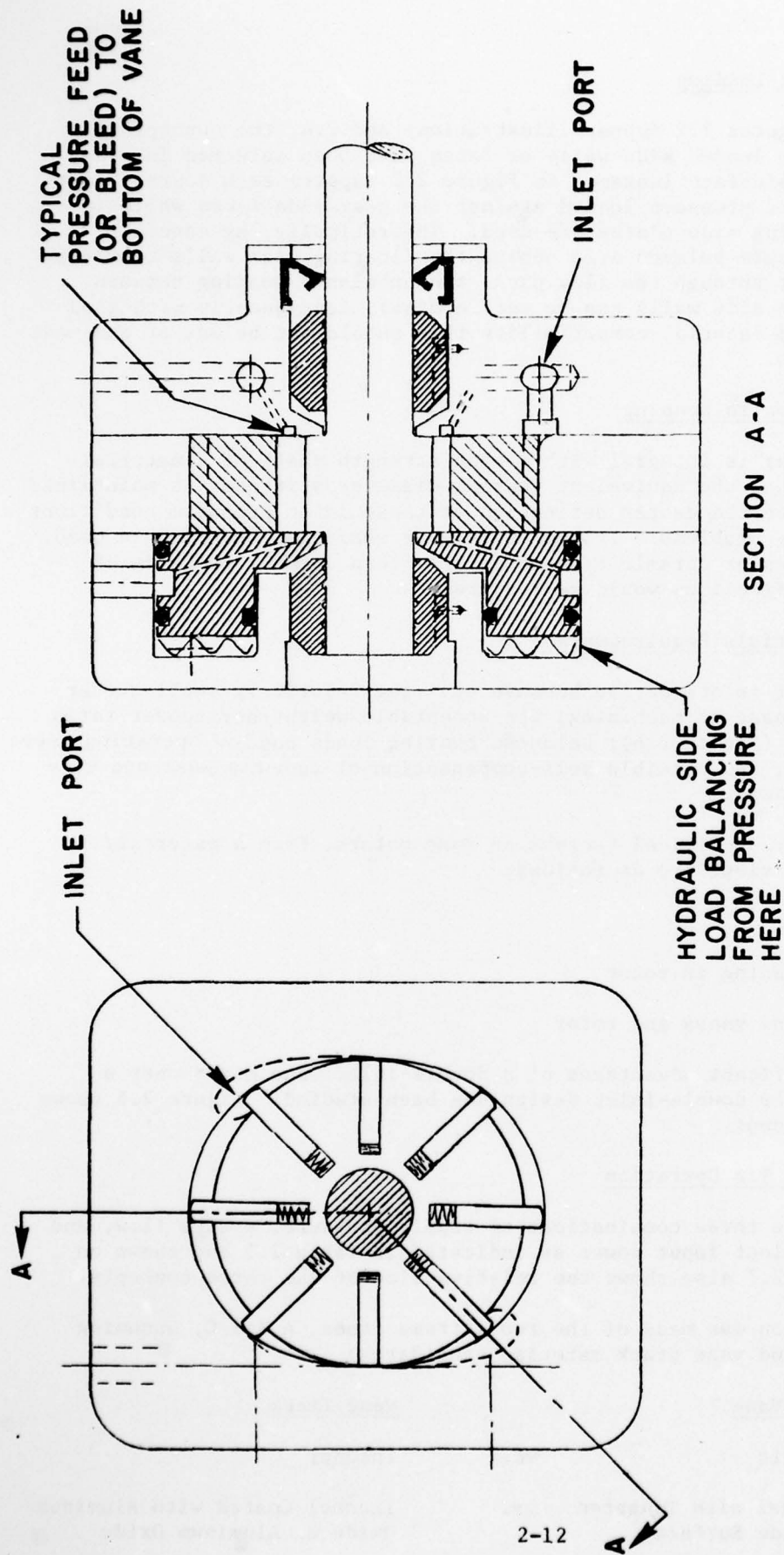
Fig. 2.6 Vane Motor – Sea Water Tools
(Double Entry Design)

TABLE 2.3

SIZING OF VANE MOTOR CONCEPTS

Track "Diameter" = 2.27"   Rotor Diameter = 2.00"

Concept	Supply Pressure psi	Q gpm	Speed rpm	Vane Width inches	Vane Thickness inches
A	1000	10	2500	0.62	0.15
B	1000	10	1250	1.24	0.15
C	1500	6.64	625	1.65	0.15

In order to obtain the tip contact stresses and resulting PV values, the following assumptions were made:

● Vanes are pressure loaded outward against the track by a combination of hydraulic pressure, centrifugal force due to vane weight and speed, and mechanical springs.

● The hydraulic pressure supplied to the bottom of the vane is metered and controlled by porting as the rotor rotates.

● A hydraulic counter-balancing force exists at the tip of the vane (see Figure 2.6) such that the outward hydraulic pressure is effective on a maximum of 50 percent of the full vane cross-sectional area. This will reduce somewhat with the vane rotational position and design, but is considered to be representative.

On these assumptions, the maximum radial tip loadings on the vane are as shown in Table 2.4.

TABLE 2.4

MAXIMUM VANE TIP LOADS

Case	A		C	
Vane Material	Plastic	Inconel	Plastic	Inconel
Spring Load lbs	0.25	0.25	0.75	0.75
Centrifugal lbs	0.40	2.42	0.07	0.40
Hydraulic lbs	46.50	46.50	186.00	186.00
TOTAL lbs	47.15	49.17	186.82	187.15

The need for good hydraulic balance is indicated by the predominance of hydraulic loading at the tip.
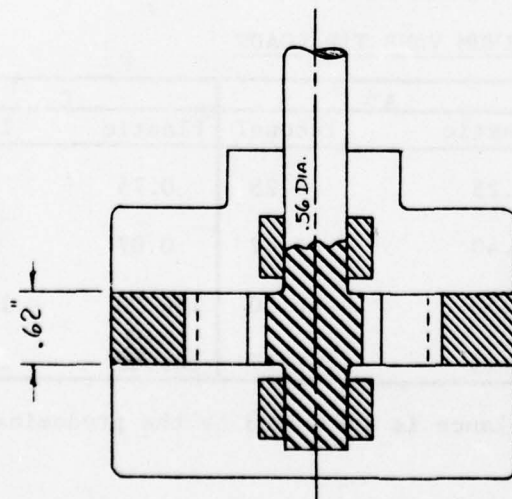
CASE A

HORSEPOWER: 5.6 HP
SPEED: 2500 RPM
FLUID PRESSURE: 1000 PSI
FLUID FLOW: 10 GPM

.56 DIA.

.62"
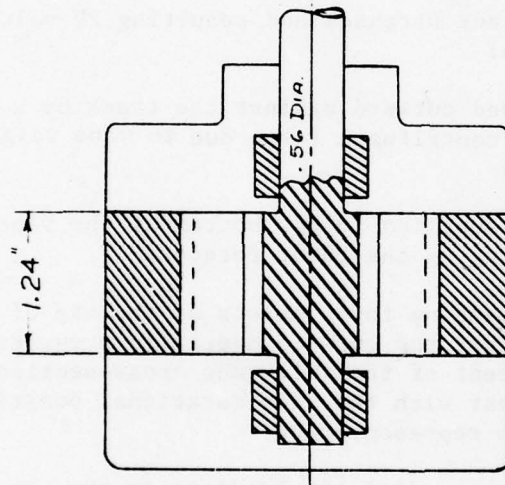
CASE B

5.6 HP
1250 RPM
1000 PSI
10 GPM

.56 DIA.

1.24"
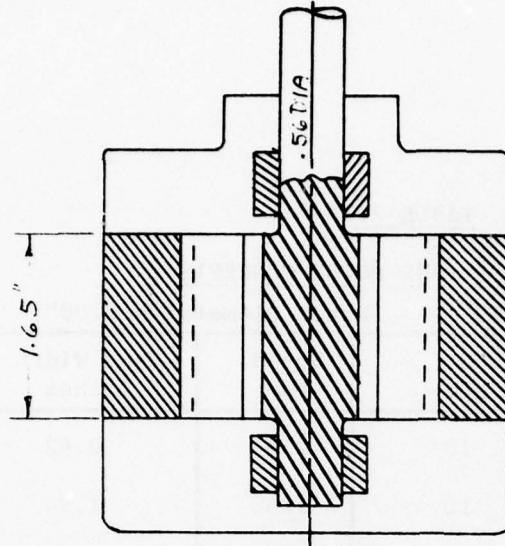
CASE C

5.6 HP
625 RPM
1500 PSI
6.64 GPM

.56 DIA.

1.65"

Figure 2.7 Vane Motor Comparison for Same Inlet Power
(Double entry designs)

2-14

2.3.2 Resultant Hertzian Stresses and PV Values at Vane Tip

It is assumed that the track and rotor are concentric over the working cycle, as shown on Figure 2.6, and, therefore, the conformity of the vane tip radius and track can be close. A track diameter of 2.27" and a vane tip "diameter" of 2.10" have been used.

The resultant Hertzian stresses (based on equations from Reference 5, see Appendix A) and PV values are shown in Table 2.5.

TABLE 2.5

VANE TIP STRESSES AND PV LEVELS

Case	A (2500 rpm, 1000 psi)		C (625 rpm, 1500 psi)	
Vane Material	Plastic	Inconel + Coating	Plastic	Inconel + Coating
Hertzian Stress P psi	1149	5450	1405	6510
Tip Velocity V fpm	1486	1486	372	372
PV Level	1,707,000	8,098,000	521,800	2,418,000

This attractiveness of a plastic vane or plastic tipped vane is evident as is the lower rotational speed. A plastic vane can be sacrificial, thus ensuring continuing performance without damage to the more expensive vane track.

2.3.3 Study of Vane Bending and PV Levels During Operation

The worse case of vane bending load occurs during start-up (Figure 2.8) with a vane in the fully extended position and with 1000 psi ΔP. Due to the concentric rotor and track design, there is no relative radial sliding occurring between vane and rotor and, consequently, no PV influence. During the actual torque-generating cycle, the loading remains on the same vane side.

Conversely, the maximum relative sliding between vane and rotor occurs when the vane is traversing a port, but in this position there is no ΔP across the vane and again no PV influence.

The maximum PV levels are generated prior to a vane reaching the high pressure inlet port, where, of course, the vane is only slightly extended to pick up pressure loading. These situations are illustrated in Figure 2.9.

2.3.4 Peak Bending Stress of Extended Vane

Concept Cases A and C from Table 2.5 are assumed. The moment loadings calculated for the two cases are given in Table 2.6.

The bending stress on the vane at X from the above moment loading and typical material properties are as shown in Table 2.7.

2-15

.135"

VANE FRICTION

F (LOAD DUE TO FLUID PRESSURE)

X

.425"

ROTATION
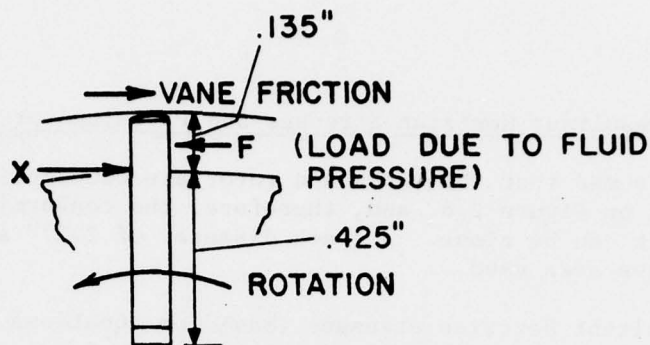
Figure 2.8 Moment Loading at Tip During Starting

TABLE 2.6

MOMENT LOADING ON VANES

Case	Vane Projected Area sq. in.	Inlet Pressure psi	F lbs	Reaction at X lbs	Moment on Tip in lbs	Balancing Moment from Tip Friction ($\mu=.1$) in lbs	Resultant Moment in lbs
A	0.084	1000	84	97.4	5.71	-.07	5.01
C	0.222	1500	334	387.4	22.70	-2.5	20.20

TABLE 2.7

BENDING STRESS ON VANE AT X

Case	Vane Bending Stress, psi	Typical Material Bending Strengths, psi	
A	2210	Plastic	26,500
C	3293	Inconel	116,000
		Aluminum Oxide	55,000

See Appendix I for bending stress equation.
It is evident that vanes of adequate strength can be selected, even in plastic, for the higher loading level of Case C (1500 psi supply pressure).

2-16

2.3.5 Calculation of Peak Pressure and PV Level of Vane Sliding in Rotor Slot

The peak radial velocity of the vane sliding in the rotor slot occurs during the rotation prior to the vane reaching the leading edge of the inlet port and with the vane extended about 0.06 inch. The pressure loading between the side of the vane and the rotor slot, assuming that the hydraulic pressure is also in the slot but not leaking around the vane, becomes somewhat complex and sensitive to the material properties of the vane and rotor. The assumed situation for these conditions is illustrated in Figure 2.9.
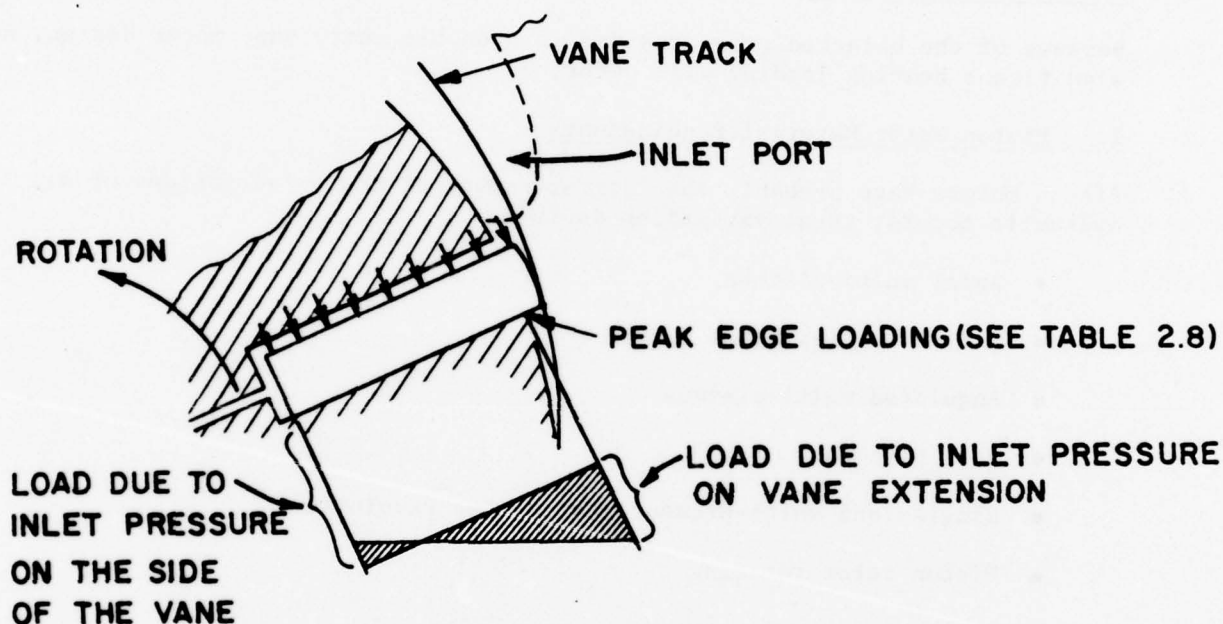
Figure 2.9. Vane Loading Diagram

Taking the conditions of Case A and Case C, the resultant peak side loadings and PV levels are as shown in Table 2.8.

TABLE 2.8

PEAK PRESSURES AND PV LEVELS IN ROTOR SLOTS

Case	A	C
Loading due to direct inlet pressure, psi	1000	1500
Edge loading due to vane extension assuming some conformity, psi	206	341
Combined edge loading, psi	1206	1823
Radial sliding velocity from layout, rpm	166	41
Peak PV Level, psi x fpm	200,200	74,750

These peak pressure and PV levels are pessimistic and are of very short time duration, occurring on the vane twice per revolution of the motor. Despite the low PV level of Case C, the Case A conditions are probably less severe for a plastic or plastic coated vane because of the lower loads and resultant material surface stress.

2.3.6 Vane End Loading

No significant vane end loading will occur due to hydraulic pressure balancing, even with a pressure loaded end plate.

2.3.7 Bearing Loading

Because of the balanced pressures due to a double entry vane motor design, no significant bearing loading will occur.

2.4 Piston Motor Material Requirements

Piston motors have probably the largest number of design variations of all hydraulic motors; these variations include:

- Axial multi-pistons

- Radial multi-pistons

- Angulated multi-pistons

- Ball pistons

- Single- and multi-pressure cycles per revolution

- Piston rotor rotating

- Piston cam track rotating

At least two designs, one of which is discussed later, have been modified and demonstrated as a sea water lubricated motor or pump.

Piston motors are attractive because of their potentially high volumetric efficiency related to the good sealing achievable with precise piston and cylinder fits, and good displacement/revolution in some designs where from 48 or 54 working strokes are possible in each motor revolution. In general, the rotor bearing loads can be balanced out although provision is necessary for the situation where a piston sticks in a cylinder to cause hydraulic unbalance.

Some of the critical areas and features of piston motors include:

- Multi-port valve plate sealing and wear

- Complexity of feed passages

- Relatively large number of precision parts

- Stresses and PV levels of piston-track interface

- Possibility of pistons sticking in cylinders

- General damage sensitivity from contaminants

For the study of piston motor material requirements, two basic types of axial piston motors have been selected (as shown in Figures 2.10 and 2.11). The first type is termed Concept I and is a nine-piston design in which the single row of pistons with slippers are in a rotor and operate against a flat, but slanting, cam plate. A pump of this type of design is used successfully as an aircraft gas turbine engine fuel pump (Figure 2.12). A second type has two variations termed Concepts II and III. This second motor type, which in a modified form has been demonstrated by N.E.L. in Scotland with sea water lubrication, consists of two rows of opposed pistons operating via rolling balls against three lobe cam tracks to give a larger number of working strokes per revolution. Figure 2.13 illustrates an industrial oil-driven motor of this type. All three concepts have been evaluated for a fluid horsepower consistent with the other motor types. Table 2.9 summarizes the design characteristics for the three concepts based on Figures 2.10 and 2.11. The detailed analysis of critical areas of these concepts has been made as discussed below.

2.4.1 Study of Piston Slipper and Track Contact Conditions - Concept I

The piston hydraulic force is taken against the flat sloping cam plate via a sliding slipper bearing in this design, as compared with the rolling ball contact on a multi-lobe track of Concepts II and III.

As shown on Figure 2.12, the slipper is fed with high pressure water from the piston via the pivot ball. There is some latitude in proportioning the outside diameter and recess diameter of the slipper to provide some pressure balance which will limit the loading on the cam track, but any possibility of slipper lift off from the track must be avoided. As discussed in Section 2.1, some hydrodynamic support will be generated between the slipper and track, but the primary support is assumed to be from the hydrostatic action as presented in Figure 2.14.

$$\text{Contact pressure between slipper and track} = \frac{P}{\cos\theta} \left[\frac{d_p^2 - d_B^2}{d_S^2 - d_B^2} \right]$$

$$= \frac{1000}{.989} \left[\frac{.5^2 - .375^2}{.75^2 - .375^2} \right]$$

$$= 263 \text{ psi}$$

Track Velocity = 2308 fpm

PV Level = 607,000 psi x fpm

2.4.2 Study of Ball Track Hertzian Stresses and "PV" Levels, Concepts II and III

An analysis has been made using Reference 8 which was derived for contact stresses between balls and ball bearing raceways. See Appendix A for stress equations.

BEARING — TRACK — SLIPPER — PISTON — BEARING

VALVE PLATE

ROTOR
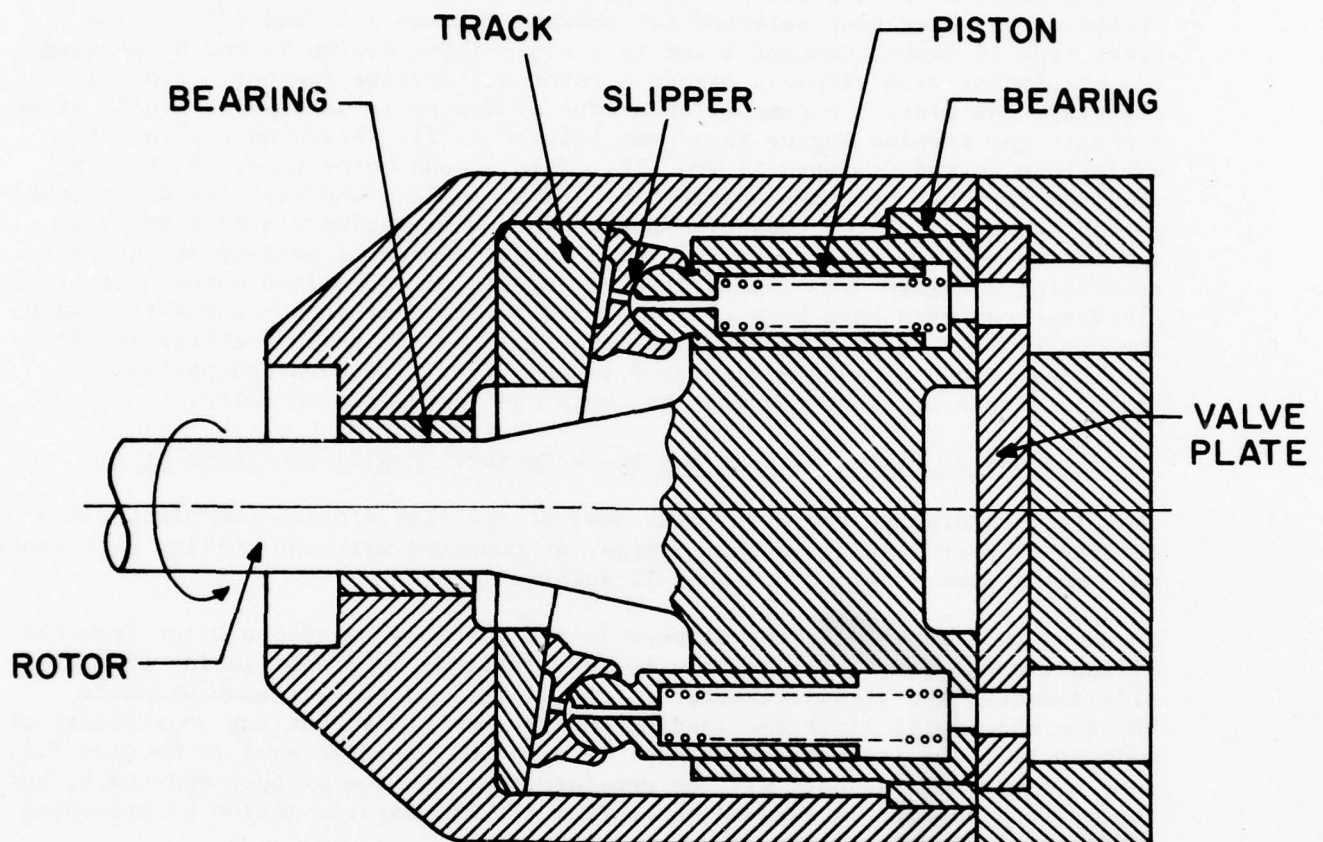
1000 PSI   10 GPM   9 PISTONS   4825 RPM

Figure 2.10   Axial Piston Motor Concept I

PISTON

BALL

ROTOR

CAM
TRACK
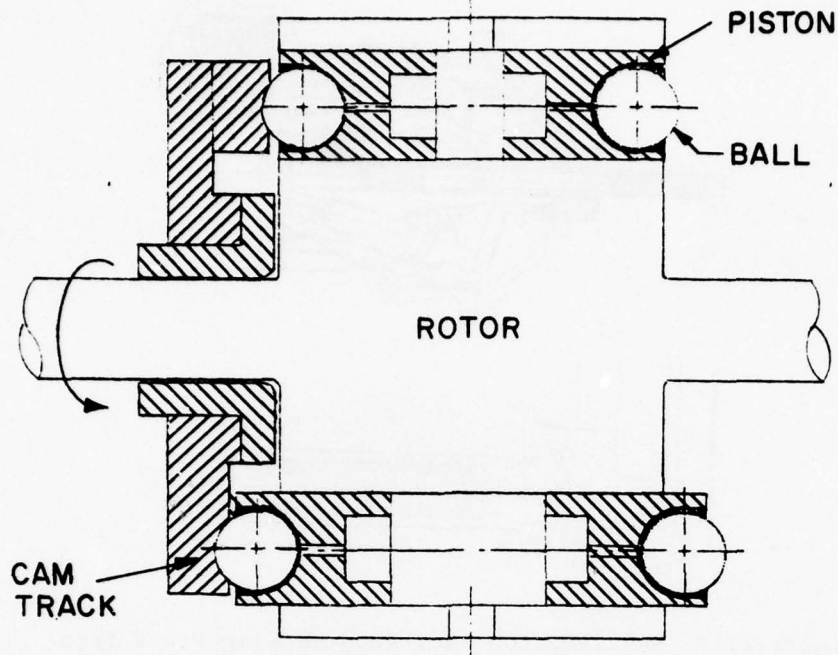
CONCEPT II

1000 PSI   10 GPM   16 PISTONS   3 LOBE CAMS   630 RPM

ROTARY VALVES
FOR FLUID
CONTROL
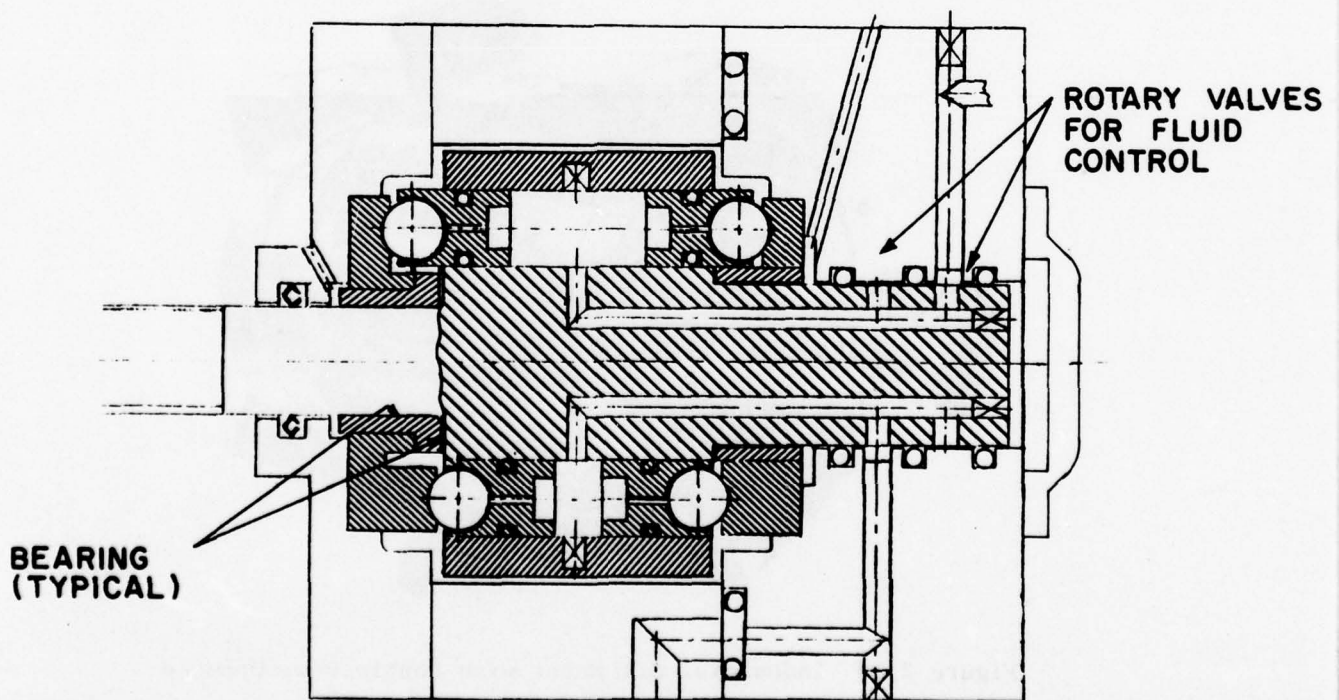
BEARING
(TYPICAL)

CONCEPT III

1200 PSI   10 GPM   16 PISTONS   3 LOBE CAMS   1060 RPM

Fig. 2.11 Axial Piston Motor Concepts

2-21
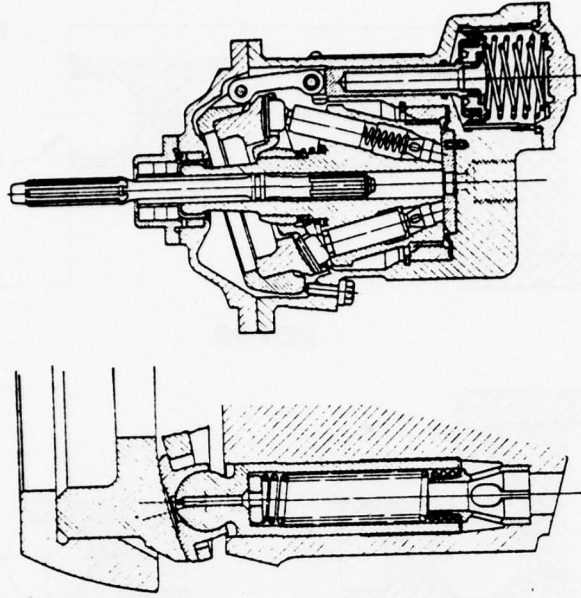
Figure 2.12   Multi-Piston Fuel Pump Showing Fluid Feed
to Slipper Bearings (Reference 6)
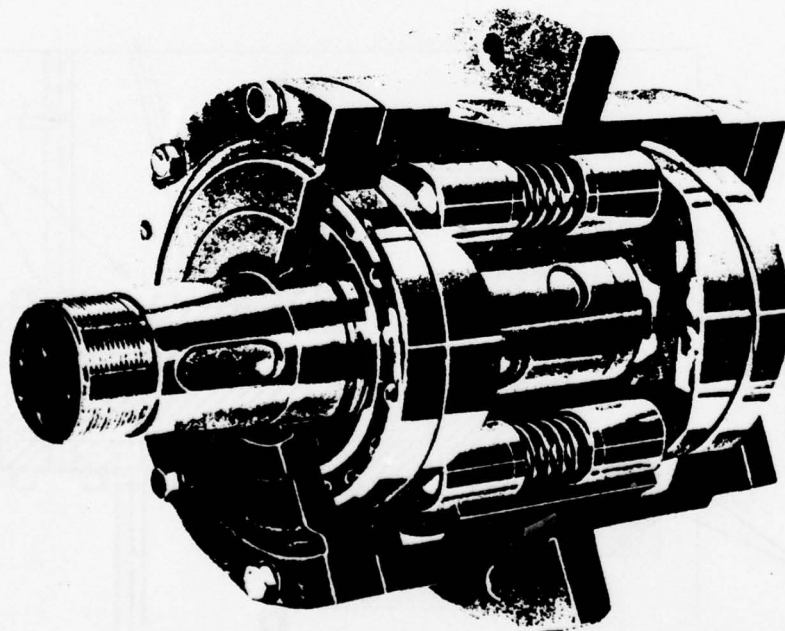
Figure 2.13   Industrial Oil Motor with Double Row, Opposed
Axial Pistons (Reference 7)

TABLE 2.9

DESIGN CHARACTERISTICS FOR PISTON MOTOR CONCEPTS

Parameter	Piston Motor Concepts		
	I	II	III
Inlet Pressure, psi	1000	1000	1200
Flow, gpm	10	10	8.28
Input Horsepower	5.8	5.8	5.8
Speed, rpm	3800	630	1060
Total Displacement, in.^{3}/rev	.608	3.682	1.805
Slipper Diameter, in.	3/4	-	-
Ball Diameter, in.	7/16	1/2	5/16
Piston Diameter, in.	1/2	5/8	7/16
Piston Stroke, in.	0.345	0.25	0.25
Number of Pistons	9	16	16
Area per Piston, in.^{2}	0.196	0.307	0.150
Number of Cam Plates	1	2	2
Number of Lobes/Cam Plate	Flat	3	3
Total Working Strokes/rev	9	48	48
Mean Track Diameter, in.	2.32	2.5	1.5
Max. Cam slope (θ) degrees	8.5 (fixed)	16.7 (sine wave)	26.56 (sine wave)
Rotor OD, in.	3.125	3.5	2.25
*Axial Piston Load (W), lbs	196	307	180
Peak Ball Load in Socket (Q), lbs	198	320	201
Peak Side Load on Piston (P) lbs	44.5	92	90
Circumferential Vel. in Track, in./sec	460	82.4	83.3
Average Ball Speed in Socket, rpm	Oscillates	3150	5088
Peak Piston Linear Velocity, in./sec	68.8	24.7	41.6

*The loads due to mechanical springs have been ignored since those are small compared to the hydraulic loading.

Two positions on the cam track for the motor Concepts II and III, detailed in Table 2.9, were selected: at the mid-point of the cam flank where the circumferential profile is practically a straight line and at the commencement of the stroke (top of the cam profile) where the curvatures have the greatest difference.

It was assumed that the cam track has a conforming curvature in the other plane such as occurs between a ball and inner race of a ball bearing.
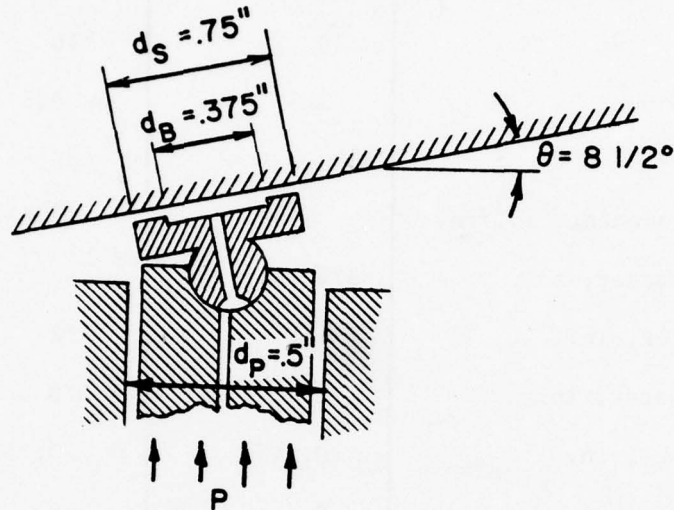
Figure 2.14   Schematic of Pressure Acting on the Slipper

The results of the analysis for the two motor concepts are given in Table 2.10

TABLE 2.10

HERTZIAN CONTACT STRESS AND PV LEVELS,
PISTON MOTOR BALL AND CAM

Position	Parameter		Concept II Larger Motor	Concept III Smaller Motor
Mid-Flank	Mean Stress	psi	174,400	199,600
	Max. Stress	psi	261,600	299,500
	Max. PV	psi x fpm	112,483,000	139,360,000
Start of Stroke	Mean Stress	psi	190,600	309,470
	Max. Stress	psi	285,800	464,200
	Max PV	psi x fpm	122,900,000	193,340,000

These contact stresses and "PV" levels appear very high, but it is of interest to review the conditions in an oil lubricated ball bearing at the inner race contact for the following representative operating conditions:

Ball Bearing, DN rating	500,000 mm x rpm
Selected Speed, rpm	10,000
Corresponding Bore Size	2 in.

2-24

Approximate Inner Race Diameter	2.25 in.
Approximate Relative Velocity of Ball to Race	3000 fpm
Typical peak Hertzian Stress	350,000 psi
Corresponding PV Rating	1,050,000,000 psi x fpm

On the same basis of analysis, the ball bearing with oil lubrication is operating at 5 to 8 times the highest PV levels calculated for the motor ball and track contact.

A rolling contact between cam track and piston is also used in other motor designs where (for example, as illustrated in Figure 2.15) rollers are needed for heavy contact loads. It is not certain that rollers could be successfully apply to a three lobe cam design particularly since slipping must inherently exist with straight rollers on a circumferential track.

2.4.3 Study of Ball Contact Conditions in Slipper or Piston Socket

In all three concepts, it is assumed that the piston ball is being fed with hydrostatic pressure from a drilling through the piston as shown in Figures 2.10 and 2.11. In the case of Concept I, oscillative motion occurs between ball and slipper, while in Concepts II and III continuous relative sliding is occurring between ball and piston socket, as defined in Table 2.9. In the analysis of socket loading and PV levels, it is assumed that the balls are retained in the sockets, such that a full 180° of contact occurs and that the socket lip acts as a seal in a manner to maintain full system pressure in the socket in order to give a hydrostatic assist. Pressures and PV levels are calculated after allowing for this hydrostatic assitance. No allowance has been made for the angulation of the load, which would tend to give somewhat greater ball loading values in the socket.

Resultant ball socket loads and PV levels are given in Table 2.11.

TABLE 2.11

BALL SOCKET LOADS AND PV LEVELS

| Parameter | Concepts | | |
	I Flat Cam Plate	II Larger Motor	III Smaller Motor
Ball Diameter, in.	7/16	1/2	5/16
Piston Diameter, in.	1/2	5/8	7/16
Piston Pressure, psi	1000	1000	1200
Load in Ball Socket, lbs	198	320	201
Ball Loading with Hydrostatic Assist, psi	320	629	1444
Resultant PV Level, psi x fpm	6560 (oscillating)	259,150	601,420
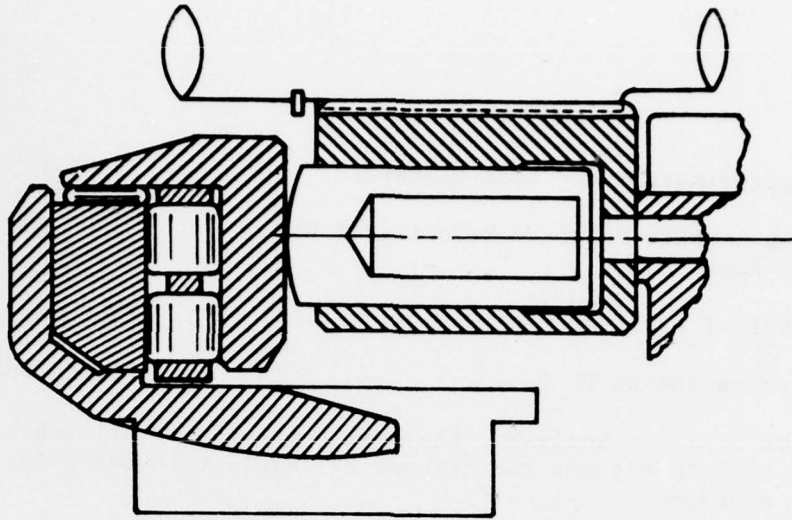
Fig. 2.15 Roller Bearing Support of Moving Cam Plate For Piston Motor
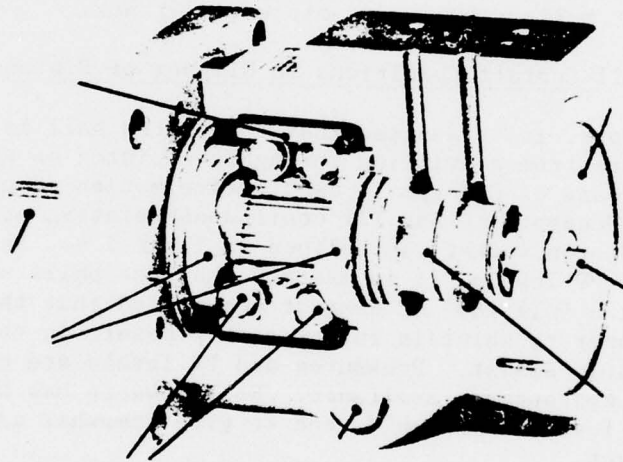
Fig. 2.16 Hydraulic Motor With Ball Pistons and Multi Lobe Track (Reference 9)
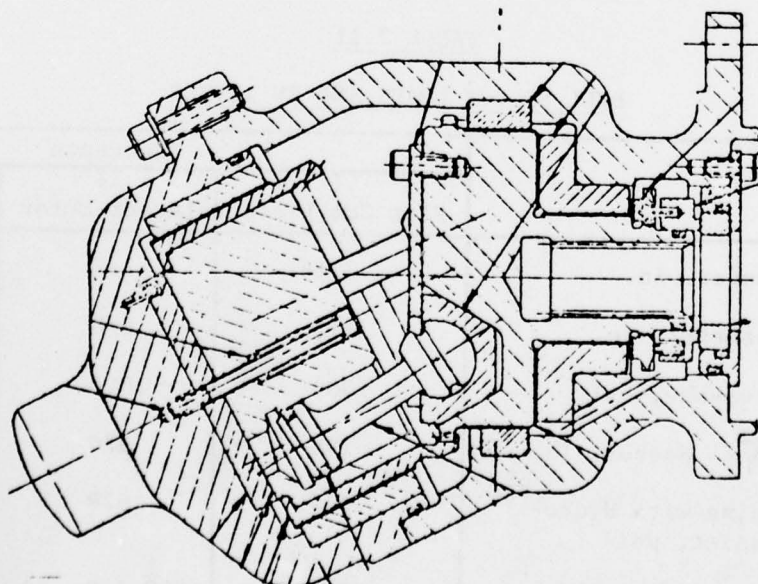
Fig. 2.17 Concept for Sea Water Motor with Spherical Pistons (Ref. 10)

TABLE 2.12

EDGE LOADING AND PV LEVELS BETWEEN PISTON AND CYLINDER

Parameter	Piston Motor Concept		
	I	II	III
Ball Side Load, lbs	44.5	92	90
Cam Angle, degrees	8.5	16.7	26.56
Load Distribution on Cylinder End at Sec A (see Fig. 2.18) lb/in.	106	355	582
Corresponding Pressure Loading at A, psi	212	570	1330
Linear Piston Velocity, fpm	344	123.5	208
Resultant PV Level, psi x fpm	72,930	70,395	276,650

TABLE 2.13

JOURNAL BEARING LOADS, MOTOR CONCEPT I

Parameter	Front Bearing	Rear Bearing
Bearing Size, diameter x L, in.	0.75 x 0.75	3.125 x 0.5
Bearing Area, in.^{2}	0.5625	1.563
Peak Load, lbs	73.3	58
Pressure Load, psi	130.3	37
Velocity, fpm	746	3108
PV Level, psi x fpm	97,200	115,000

2.4.4 Study of Edge Loading and PV Levels Between Piston and Cylinder

The three motor concepts have been studied from layout drawings to determine the edge loading between piston and cylinder by resolving the forces generated at the appropriate cam angles. In the case of multi-lobe cams of Concepts II and III, the mid-flank cam position was used to obtain maximum angle and linear velocity of the pistons in the cylinders.

A loading profile has been assumed, as illustrated below, in order to determine the load distribution on the piston. No allowance has been made for modifications to pressure profile of working fluid by piston cocking. It will be appreciated that introducing a piston ring seal could affect the lubrication at the edge of the cylinder.

ZONES OF LOAD DISTRIBUTION
BASED ON REACTIONS TO P
AND PISTON CLEARANCE
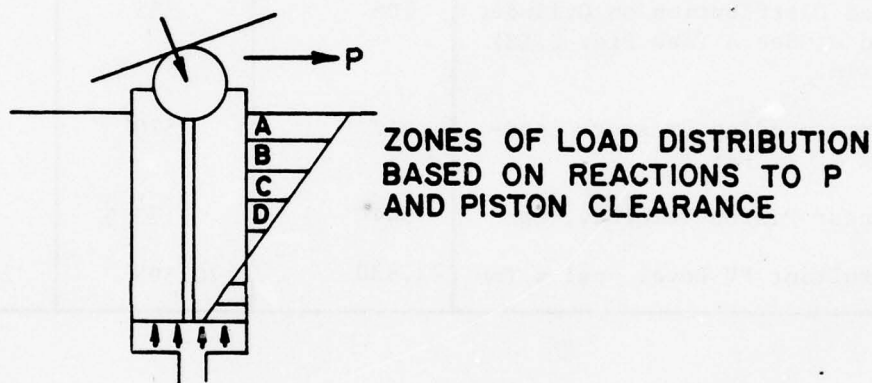
Figure 2.18. Assumed Loading Profile on the Piston

A study of Table 2.12 indicated that the loading and PV levels can be held to acceptable values by careful motor design. Some hydrodynamic lubrication assistance can be anticipated in Concepts II and III due to the rotational speed of the ball, but this has not been included.

Two further variations on the ball and piston designs in hydraulic motors are shown in Figure 2.16 and 2.17. The oil motor design in Figure 2.16 is simple in that it utilizes a ball for the actual piston. The line contact of the ball in the cylinder may present problems with water due to loading and minimal sealing.

The concept in Figure 2.17 is an angulated motor design which had been proposed for a sea water lubricated motor. It utilizes a spherical piston with an O-ring seal.

2.4.5 Motor Bearing Loading

The journal bearing loading reactions resulting from all the pistons acting against the cam plate have been calculated for the flat cam plate motor Concept I, and the results are given in Table 2.13 together with the bearing pressures and PV levels.

The radial bearing loading of the multi-piston three lobe cam type motor, Concepts II and III, is more complex because of the multi-piston action. An analysis shows that this action does result in significant inherent balancing.

The axial bearing load of motor Concept I occurs on the valve plate where there is considerable latitude to establish low loading within the limitation of providing an adequate port sealing loading on the plate.

The axial bearing load of motor Concepts II and III is inherently balanced by the opposed piston. Provision must be made, however, for the possibility of a piston lock-up which would change the hydraulic balance in any piston motor design. Lock-up of one piston in Concept III would result in a thrust bearing pressure loading of 306 psi and a PV level of 63,700 psi x fpm. Similarly, the radial bearing loading of these motors would increase with a piston lock-up.

2.5 Summary of Material Operating Requirements for All Motor Types

To conclude Chapter 2 motor analysis studies, Table 2.14 has been compiled to conveniently summarize the most critical components and their material operating requirements. This data can be used to measure the suitability of materials identified in Chapter 3.

TABLE 2.14

SUMMARY OF TYPICAL OPERATING CONDITIONS FOR ALL MOTOR TYPES
(all for constant input fluid HP)

		N rpm	P psi	PV psi x fpm
Gear Motor				
Gear Mesh				
Steel/Steel (External)		2500	102,500	56,890,000
Steel/Plastic (External)		2500	11,800	6,550,000
Steel/Plastic (Internal)		2500	7,160	1,475,000
Bearing (Radial)		2500	750	367,500
Vane Motor				
Vane Tip				
Plastic Vane	Condition A	2500	1,149	1,707,000
Inconel Vane		2500	5,450	8,100,000
Plastic Vane	Condition C	625	1,405	521,800
Inconel Vane		625	6,510	2,418,000
Vane Side-Sliding				
Condition A		2500	1,206	200,200
Condition C		625	1,823	74,750
Piston Motor				
	Concepts			
Track Contact	I (slipper sliding)	3800	263	607,000
	II (ball rolling)	630	285,800 (max)	122,900,000
	III (ball rolling)	1060	464,200	193,340,000
Piston Edge	I	3800	212	72,930
	II	630	570	70,395
	III	1060	1,330	276,650
Ball In Socket	I	Ball in Socket Oscillating	320	6,560
	II	3150	629	259,150
	III	5088	1,444	601,420
Bearings - Radial	I	3800	130	97,200
Bearings - Axial	III (with piston lock-up)	1060	306	63,700

3.0 MATERIAL SELECTION AND THEIR PROPERTIES

An in-depth survey of the materials literature was conducted to select materials suitable for piston, gear, and vane types of motors, based on stresses and velocities of their critical components and locations. The material properties of the selected materials were researched and tabulated. If the wear, friction, and corrosion properties in the simulated conditions were not available, then tests were conducted.

3.1 Properties of Lubricating Media

The subject motor would use sea water as a process fluid. The composition and tribological properties of sea water may vary slightly from sea to sea. Therefore, an ASTM standard synthetic sea salt (supplied by Lake Products Company, Ballwin, Mo.) was obtained, and it was mixed in water in the proportion of 5-1/2 ounces per gallon, to make synthetic sea water. This synthetic sea water was used in the tests to simulate sea water. The specifications of the sea salt are given in Table 3.1. Sea salt is a simulated salt mix containing elements found in natural sea water in quantities greater than 0.0004 percent.

The viscosity of the sea water is very low compared to hydraulic oils. The materials selection of the motor components does depend on the lubricating media. The viscosity of the fluids changes with temperature and pressure. Effect of pressure and temperature on the viscosity of the sea water and hydraulic oils is shown in Figures 3.1 and 3.2. The data show that the viscosity of sea water is very low compared to that of the hydraulic oils. The viscosity of sea water decreases somewhat with an increase in temperature, and it is practically insensitive to pressure. It is felt that since viscosity does not change with pressure, there will be no squeeze film effect.

3.1.1 Effect of Additives

Sea water is a poor lubricant. As discussed earlier, the PV (load x velocity) requirements for the materials can be high. It would be very helpful if certain additives could be used to improve the lubricity. It is desirable that the percentage amount of these additives should be as small as possible, and the additives should be bio-degradable, since the output of the motor would be dumped into the ocean. In the studies, if no combination for some motor component performed well, then the tests with additives were run to see if the performance could be improved.

Hampson and Naylor [12] found that turbulent fluid friction can be reduced up to 45 percent by adding 5 to 200 μg/g of high-molecular weight polymer, Polyox WSR 301 (approximate molecular weight = 4×10^6) to the water. Their study showed that optimum concentration was 50 μg/g. It was also observed that degradation of the polymer by mechanical shear was quite rapid.

The degradation of the polymer would not be a problem in the motor application since the used water mixture would be dumped and fresh mixture would be pumped continuously.

Polyox resins are easily wettable. The desired amount of the powder can be mixed in the water with some mechanical agitation. To insure proper mixing of resin in sea water, one unit of additive resin is mixed with five units of anhydrous isopropanol and the mixture is stirred to disperse the particles. The resulting dispersion can then be added to salt water and agitated. The mixture can further be mixed with a mechanical stirrer.

3-1

TABLE 3.1

SPECIFICATIONS OF SYNTHETIC SEA WATER
ASTM D-1141-52

Mixture contains U.S.P., N.F.,and High Grade Commercial Salts.

SUBSTITUTE OCEAN WATER SALT

$NaCl$	(99.9% Pure)	58.490%
$MgCl_2 6H_2O$	(99% Pure)	26.460%
Na_2SO_4	(99.97% Pure)	9.750%
$CaCl_2$	(94-97% Pure)	2.765%
KCL	(99.95% Pure)	1.645%
$NaHCO_3$	(99% Pure)	0.477%
KBr	(99% Pure)	0.238%
H_3BO_3	(99.9% Pure)	0.071%
$SrCl_2 .6H_2O$	(99% Pure)	0.095%
NaF	(99% Pure)	0.007%

Density of Sea Water equals 1.025 at 15° C.

3-2
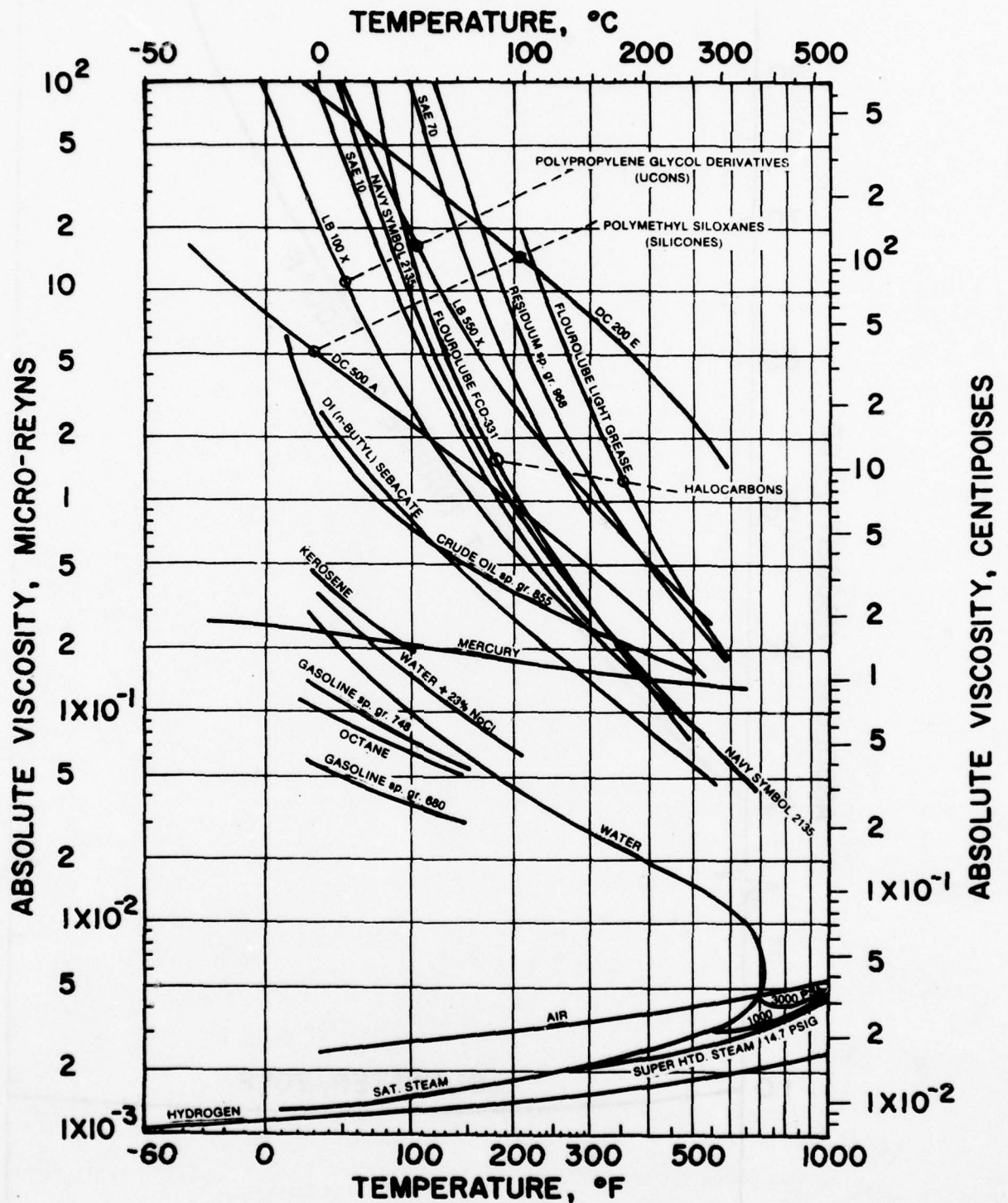
Figure 3.1 Viscosity-Temperature Chart Showing Relative
Viscosities of a Number of Fluids at Various
Temperatures (Reference 11)
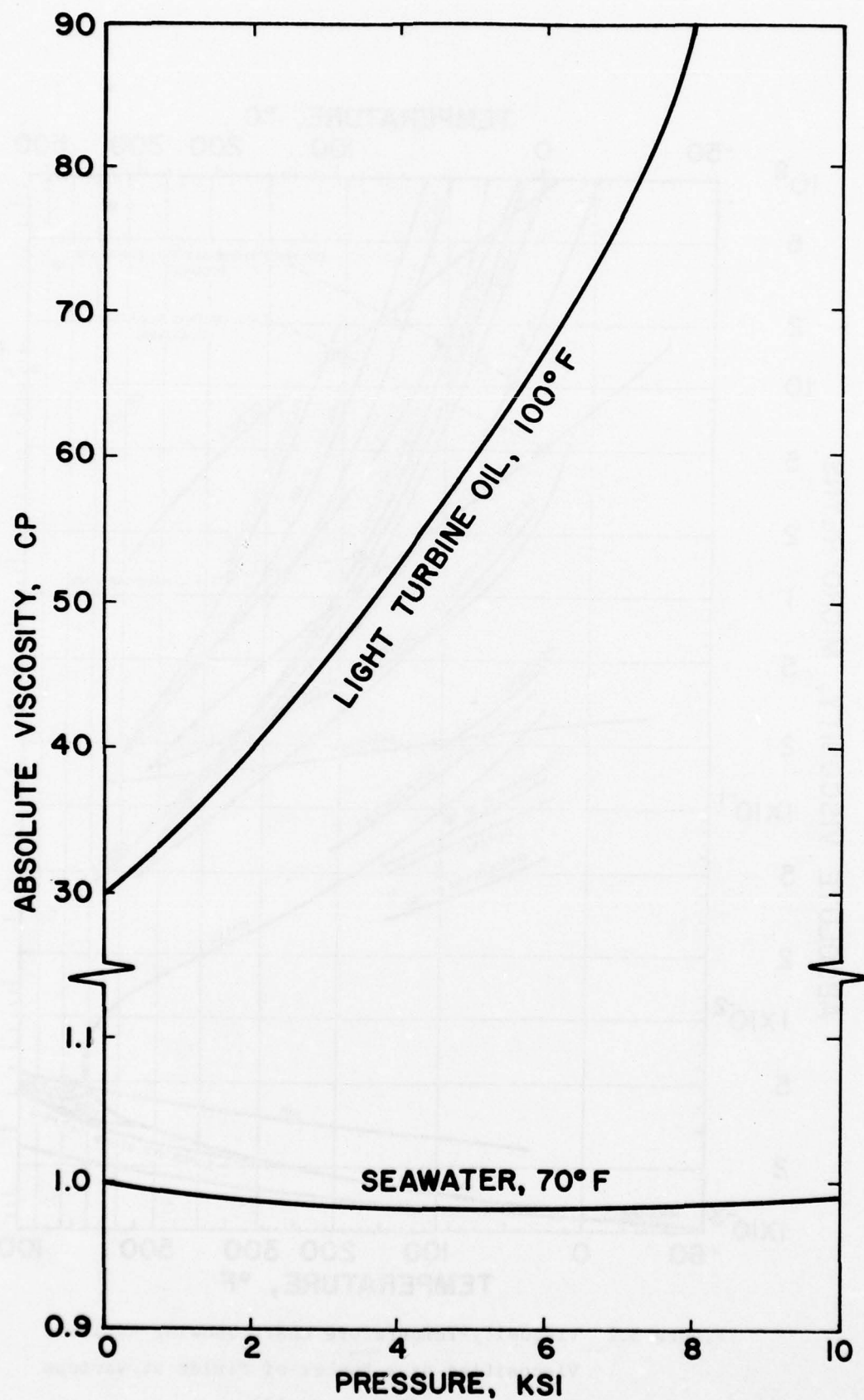
Figure 3.2   Viscosity-Pressure Chart of Sea Water
and Hydraulic Oil

Polyox coagulant has an approximate molecular weight of 5×10^6 and was selected for the tests. Some technical data supplied by Union Carbide [13] on different grades of Polyox resins are presented in Figure 3.3.

The additives were only used when it was considered really necessary, because they are cumbersome to use and undesirable.

3.2 Material Survey

There is a considerable amount of wear data available in the literature on plastics rubbing against metals in the water-lubricated conditions (e.g., water-lubricated bearings). There is some wear data available on metal-ceramic, metal-metal, and ceramic-ceramic combinations. Major manufacturers were contacted to obtain more technical data and to learn about any new materials relevant to the sea water motor application.

A review of published wear data on material combinations is presented in Table 3.2. The mechanical, thermal, and electrical properties of standard plastics are listed in Modern Plastics Encyclopedia. It is felt that the properties of the plastics may vary appreciably from manufacturer to manufacturer. Wherever possible, the available properties of pertinent materials were obtained from the vendor who had supplied the test pieces. For comparisons, the properties of leading plastic candidates are presented in Table 3.3. Many metals are available which are corrosion-resistant and have good anti-galling characteristics. Based on past experience, contact with the vendors and the review of published literature (References 25, 30, and 31), the potentially promising corrosion-resistant metals were selected and are tabulated with their mechanical properties supplied by the manufacturers, in Table 3.4. The chemical compositions of the metals are presented in Table 3.5. As discussed later, little emphasis was placed on ceramic/cermets due to their brittleness. Some ceramic, cermets, and composites were studied for suitability and their mechanical and thermal properties are listed in Table 3.6.

3.3 Final Selection of Materials for Screening Tests

3.3.1 General Discussion and Selection Criteria

Plastics are ideal materials in sea water due to their inertness. However, plastics do not have good mechanical properties compared to most metals. Many plastics have a tendency to swell when submerged in sea water. They deform rather easily when subjected to load at high temperatures, i.e., they have low heat deflection temperature. Metal-plastic combinations were preferred wherever possible, as they usually do not have galling problems as many metal-metal combinations have. Some metals also have excellent corrosion resistance and have superior mechanical properties. Wherever plastics satisfy mechanical requirements, it was decided that metal-plastic combinations should be used. Since plastics do not have good thermal dissipating properties, a plastic-plastic combination was not recommended as there may be excessive heat build up, even in water, which may result in considerable loss in mechanical strength. In some parts, the mechanical requirements or tolerances desired at the interface may dictate the usage of metal-metal or ceramic combinations. Plastic coatings, if feasible on metal substrates, may also satisfy mechanical requirements. In a material study done by Bedford, et al. [14], it was suggested that ceramics, carbides, block carbon graphite, and some alloys, while potentially good from an anti-galling and load bearing point of view, may be too brittle for applications in a portable unit which would be subjected to rough handling or impact shocks. Also, graphite is a strong promoter of galvanic corrosion
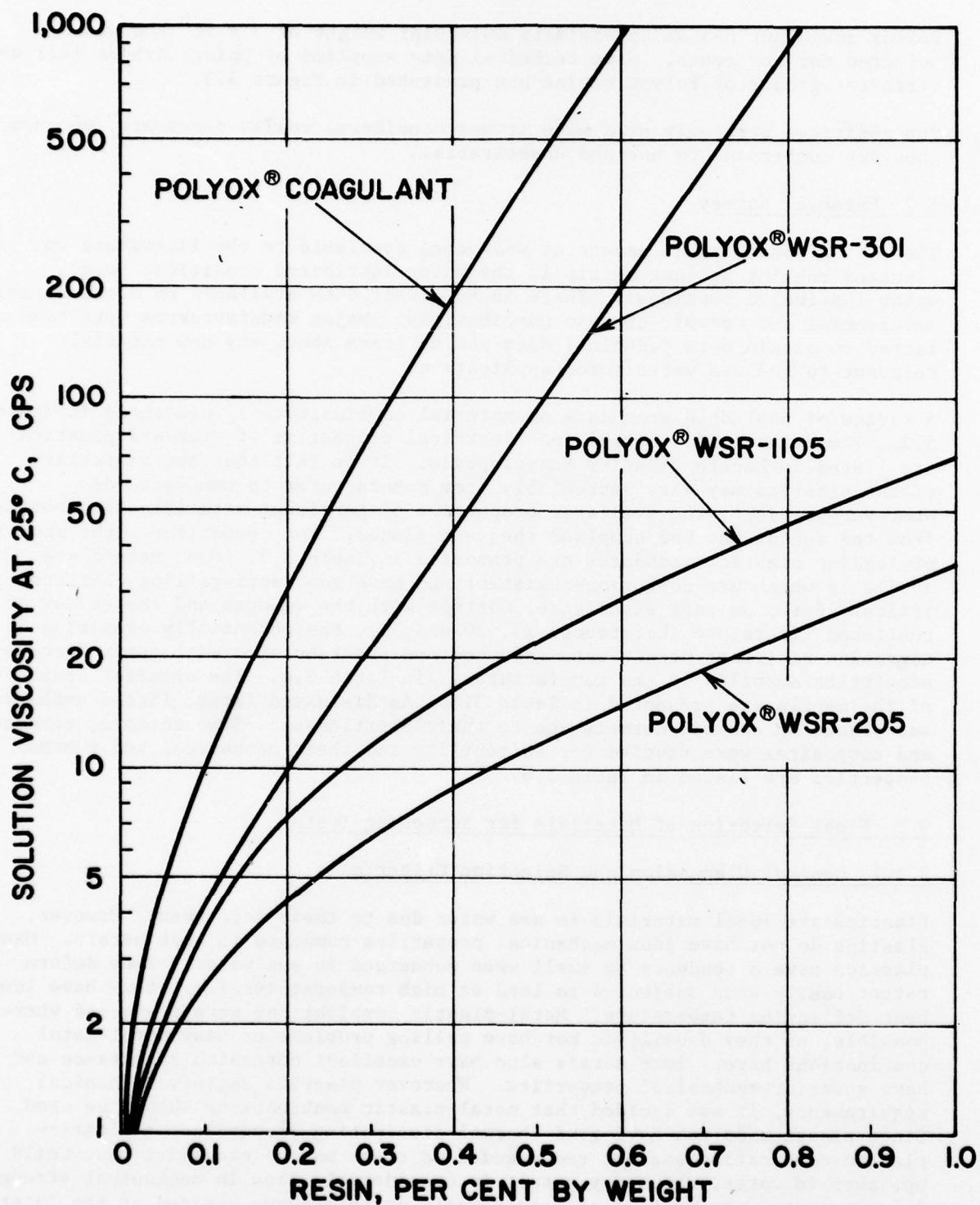
Figure 3.3 Solution Viscosity Versus Polyox® Resin Concentration

TABLE 3.2

REVIEW OF PUBLISHED MATERIAL COMBINATIONS FRICTION AND WEAR TEST DATA

3.2.1 Polyethylene

Test Material Pair	Mode of Lubrication	Coefficient of Friction	Wear Loss	Comments	Test Period	Description of the Test Apparatus
1. HD Polyethylene vs. "R" Monel[15]	Water	0.051	85 x 10^{-4} cc	Smooth Running	1 hour	Thrust-washer wear tester (continuous rubbing 577 psi and 500 rpm (139 fpm)
2. 25% Cu, 15% Pb and 60% HD Polyethylene vs. "R" Monel[15]	Water	0.048	58 x 10^{-4} cc	Smooth Running	1 hour	Thrust-washer wear tester (continuous rubbing 577 psi and 500 rpm (139 fpm)
3. 15% Cu, 10% Pb and 75% HD Polyethylene vs. "R" Monel[15]	Water	0.050	57 x 10^{-4} cc	Smooth Running	1 hour	Thrust-washer wear tester (continuous rubbing 577 psi and 500 rpm (139 fpm)
4. 25% MoS2-graphite (10:1), 75% HD Polyethylene vs. "R" Monel[15]	Water	0.064	35 x 10^{-4} cc	Smooth Running	1 hour	Thrust-washer wear tester (continuous rubbing 577 psi and 500 rpm (139 fpm)
5. 40% MoS2-graphite (10:1), 75% HD Polyethylene vs. "R" Monel[15]	Water	0.046	23 x 10^{-4} cc	Smooth Running	1 hour	Thrust-washer wear tester (continuous rubbing 577 psi and 500 rpm (139 fpm)
6. Ultra HD Polyethylene vs. "R" Monel	Water	0.079	20 x 10^{-4} cc	Smooth Running	1 hour	Thrust-washer wear tester (continuous rubbing 577 psi and 500 rpm (139 fpm)
7. 5% graphite-fiber filled Polyethylene vs. "R" Monel[15]	Water	0.046	12 x 10^{-4} cc	Smooth Running	1 hour	Thrust-washer wear tester (continuous rubbing 577 psi and 500 rpm (139 fpm)
8. 50% bronze-fiber-filled Polyethylene vs. "R" Monel[15]	Water	0.023	5 x 10^{-4} cc	Smooth Running	1 hour	Thrust-washer wear tester (continuous rubbing 577 psi and 500 rpm (139 fpm)
9. Ultra-HD Polyethylene vs. "R" Monel[15]	Synthetic Sea Water	-	0.011 in.	Quiet	80 hours	Sleeve bearing operation 577 psi, 15.3 fpm (19 rpm)
10. Graphite-fiber-filled HD Polyethylene vs. "R" Monel[15]	Synthetic Sea Water	-	0.088 in.	Quiet	80 hours	Sleeve bearing operation 577 psi, 15.3 fpm (29 rpm)
11. HD Polyethylene (708) vs. Monel[16]	Water	0.13	1.18 u in./ft of travel			Continuous sliding test, load 6 lbs.
	Dry	0.16				Continuous sliding test, load 6 lbs.
12. LD Polyethylene (718) vs. Monel[16]	Water	0.13	3.31 u in./ft of travel			Continuous sliding test, load 6 lbs.
	Dry	0.63				Continuous sliding test, load 6 lbs.
13. LD Polyethylene (718) with 50% Regal 300 and 5% Dicumyl Peroxide (Di-cup) vs. Monel16	Water	0.26	2.16 u in./ft of travel			Continuous sliding test, load 6 lbs.
	Dry	0.5				
14. LD Polyethylene (718) with 50% Sterling MT-FF and 5% Di-cup16	Water	0.22	2.46 u in./ft of travel			Continuous sliding test load 6 lbs.
	Dry	0.48				
15. HMWPE vs. Hastelloy C [17]	Sea Water	0.060	10.5 x 10^{-4} cc	Smooth Running	1 hour	Thrust-washer wear tester (continuous rubbing) 577 psi and 500 rpm (139 fpm)
vs. Titanium	Sea Water	0.085	9.2 x 10^{-4} cc	Smooth Running	1 hour	
vs. Inconel 625	Sea Water	0.061	9 x 10^{-4} cc	Smooth Running	1 hour	

3.2.1 Polyethylene cont'd

Test Material Pair	Mode of Lubrication	Coefficient of Friction	Wear Loss	Comments	Test Period	Description of the Test Apparatus
16. HDPE vs. Hastelloy C [17]	Sea Water	0.061	12.5×10^{-4} cc	Smooth Running	1 hour	Thrust-washer wear tester (continuous rubbing) 577 psi and 500 rpm (139 fpm)
vs. Titanium	Sea Water	0.068	5.05×10^{-4} cc	Smooth Running	1 hour	
vs. Inconel 625	Sea Water	0.055	3.5×10^{-4} cc	Smooth Running	1 hour	
17. XLPE vs. Hastelloy C [17]	Sea Water	0.09	10.9×10^{-4} cc	Smooth Running	1 hour	Thrust-washer wear tester (continuous rubbing) 577 psi and 500 rpm (139 fpm)
vs. Titanium	Sea Water	0.094	12.1×10^{-4} cc	Smooth Running	1 hour	
vs. Inconel 625	Sea Water	0.075	7.2×10^{-4} cc	Smooth Running	1 hour	
18. 30% Kaolin-filled PE vs. Hastelloy C [17]	Sea Water	0.066	10.2×10^{-4} cc	Smooth Running	1 hour	Thrust-washer wear tester (continuous rubbing) 577 psi and 500 rpm (139 fpm)
vs. Titanium	Sea Water	0.044	3.1×10^{-4} cc	Smooth Running	1 hour	
vs. Inconel 625	Sea Water	0.039	6.2×10^{-4} cc	Smooth Running	1 hour	
19. 5% Carbon black, 40% Glass-fiber, 5% CTBN-filled HDPE vs. Inconel 625 [17]	Sea Water	0.033	1.4×10^{-4} cc		1 hour	Thrust-washer wear tester, 577 psi, 500 rpm (139 fpm)
vs. Hastelloy C	Sea Water	0.048	7.8×10^{-4} cc		1 hour	
vs. Titanium	Sea Water	0.072	2.0×10^{-4} cc		1 hour	
20. 30% Glass-fiber filled HDPE vs. Inconel 625	Sea Water	0.028	1.4×10^{-4} cc		1 hour	Thrust-washer wear tester, 577 psi, 500 rpm (139 fpm)
vs. Hastelloy C	Sea Water	0.045	5.6×10^{-4} cc		1 hour	
vs. Titanium	Sea Water	0.175	310×10^{-4} cc		1 hour	
21. 30% Carbon black, 5% CTBN-filled HDPE vs. Inconel 625 [17]	Sea Water	0.078	2.1×10^{-4} cc		1 hour	Thrust-washer wear tester, 577 psi, 500 rpm (139 fpm)
vs. Hastelloy C	Sea Water	0.080	3.7×10^{-4} cc		1 hour	
vs. Titanium	Sea Water	0.087	3.9×10^{-4} cc		1 hour	
22. 10% SIC, 15% PTFE-filled HDPE vs. Inconel 625 [17]	Sea Water	0.050	3×10^{-4} cc		1 hour	Thrust-washer wear tester, 577 psi, 500 rpm (139 fpm)
vs. Hastelloy C	Sea Water	0.045	4.9×10^{-4} cc		1 hour	
vs. Titanium	Sea Water	0.049	18.5×10^{-4} cc		1 hour	
23. 15% Glass fibers, 5% MoS$_2$ filled HDPE vs. Inconel 625 [17]	Sea Water	0.037	3.7×10^{-4} cc		1 hour	Thrust-washer wear tester, 577 psi, 500 rpm (139 fpm)
vs. Titanium	Sea Water	0.051	213×10^{-4} cc		1 hour	
24. PE vs. PE [18]	Water	0.29	5×10^{-5} in/ft of travel	Swelling during immersion .001 in./in. in 6 mo.		Continuous sliding tests 52 fpm (100 rpm), 4 lb/in. on 2" φ bearing.
25. HMWPE vs. Manganese Bronze [19]	Sea Water	0.068	15 cc/1000 hours	Quiet	1 hour	Thrust-washer wear tester (continuous rubbing) 577 psi and 40 rpm (10 fpm)
26. HMWPE vs. 304 ss [19]	Sea Water	0.051	23 cc/1000 hours	Quiet	1 hour	Thrust-washer wear tester (continuous rubbing) 577 psi and 40 rpm (10 fpm)

3-8

3.2.2 Polyimide

Test Material Pair	Mode of Lubrication	Coefficient of Friction	Wear Loss	Comments	Test Period	Description of the Test Apparatus
1. Polyimide vs. "R" Monel [15]	Water	0.17	Excessive	Violent Stick-Slip	1 hour	Thrust-washer wear tester 577 psi and 500 rpm (139 fpm)
2. 15% Graphite-filled Polyimide vs. "R" Monel [15]	Water	0.030	19×10^{-4} cc	Smooth Running	1 hour	Thrust-washer wear tester 577 psi and 500 rpm (139 fpm)
3. 30% Graphite PTFE-filled Polyimide vs. "R" Monel [15]	Water	0.035	15×10^{-4} cc	Smooth Running	1 hour	Thrust-washer wear tester 577 psi and 500 rpm (139 fpm)
4. PTFE-filled Polyimide vs. "R" Monel [15]	Synthetic Sea Water		0.003 in.	Quiet	80 hours	Sleeve Bearing operation 577 psi, 15.3 fpm (39 rpm)
5. Graphite-filled Polyimide vs. "R" Monel [15]	Synthetic Sea Water		0.003 in.	Quiet	80 hours	Sleeve Bearing operation 577 psi, 15.3 fpm (39 rpm)
6. Polyimide vs. Inconel 625 [17]	Synthetic Sea Water	0.072	1.4×10^{-4} cc		80 hours	Thrust-washer wear tester 577 psi and 500 rpm (139 fpm)
7. Polyimide vs. Titanium [17]	Synthetic Sea Water	0.172	Broke			Thrust-washer wear tester 577 psi and 500 rpm (139 fpm)

3.2.3 PTFE

Test Material Pair	Mode of Lubrication	Coefficient of Friction	Wear Loss	Comments	Test Period	Description of the Test Apparatus
1. Glass-filled PTFE vs. "R" Monel [15]	Water		Excessive	Heavy extrusion test terminated after 5 minutes	5 min.	Thrust-washer wear tester 577 psi, 500 rpm (139 fpm)
2. PTFE-lead-bronze composite vs. "R" Monel [15]	Water	0.13	Excessive	Smooth Running	1 hour	Thrust-washer wear tester 577 psi, 500 rpm (139 fpm)
3. Bronze-filled PTFE vs. "R" Monel [15]	Water	0.18	92×10^{-4} cc	Smooth Running	1 hour	Thrust-washer wear tester 577 psi, 500 rpm (139 fpm)
4. PTFE-filled acetal vs. "R" Monel [15]	Water	0.041	47×10^{-4} cc	Smooth Running	1 hour	Thrust-washer wear tester 577 psi, 500 rpm (139 fpm)
5. PTFE-lead-bronze composite vs. "R" Monel [15]	Synthetic Sea Water		0.005 in.	Quiet	80 hours	Sleeve bearing operation 577 psi, 15.3 fpm (39 rpm)
6. PTFE-filled Acetal [15]	Synthetic Sea Water		Excessive	Quiet	80 hours	Sleeve bearing operation 577 psi, 15.3 fpm (39 rpm)
7. Polyimide-filled PTFE vs. Titanium [17]	Synthetic Sea Water	0.095	19.2×10^{-4}		1 hour	Thrust-washer wear tester 577 psi, 500 rpm (139 fpm)
8. Polyimide-filled PTFE vs. Hastelloy C [17]	Synthetic Sea Water	0.061	4.7×10^{-4} cc		1 hour	Thrust-washer wear tester 577 psi, 500 rpm (139 fpm)
9. Polyimide-filled PTFE vs. Inconel 625 [17]	Synthetic Sea Water	0.096	7.1×10^{-4} cc		1 hour	Thrust-washer wear tester 577 psi, 500 rpm (139 fpm)
10. PTFE lining vs. 440 C stainless [20]	Dry	0.06	0.006 in.	Increase in speed decreases wear life.	10,000 cycles	Fabric lined oscillating spherical bearings, 28900 psi; 10 cycles/min.; 50° oscillation
	Sea Water	0.055	0.005 in.		10,000 cycles	
11. 30% Carbon fiber reinforced Ethylene-TFE vs. 1040 steel [21]	Dry	0.22	17×10^{-10} in.^{3}min/ft/ lb/hr	Carbon behaves not only reinforcing filler but as an internal lubricant		Thrust-washer wear tester, 50 ft/min, 60 psi

3.2.3 PTFE continued

Test Material Pair	Mode of Lubrication	Coefficient of Friction	Wear Loss	Comments	Test Period	Description of Test Apparatus
12. 30% Glass fiber reinforced Ethylene-TFE vs. 1040 steel [21]	Dry	0.36	20×10^{-10} in.^{3} min/ft/lb/hr			Thrust-washer wear tester 50 ft/min, 40 psi
13. Ethylene-TFE vs. 1040 steel [21]	Dry	0.40	$6,000 \times 10^{-10}$ in.^{3} min/ft/lb/hr			Thrust-washer wear tester 50 ft/min, 40 psi
14. Polyvinylidene Fluoride TFE vs. 1040 steel [21]	Dry	0.70	$>2000 \times 10^{-10}$ in.^{3}min/ft/lb/hr			Thrust-washer wear tester 50 ft/min, 40 psi
15. 30% Carbon fiber reinforced Polyvinylidene Flouride vs. 1040 steel [21]	Dry	0.13	13×10^{-10} in.^{3}min/ft/lb/hr			Thrust-washer wear tester 50 ft/min, 40 psi
16. PTFE vs. 304 SS [19]	Sea Water	0.071	2cc/1000 hours	Quiet	1 hour	Thrust-washer wear tester, 577 psi and 40 rpm (10 fpm)
3.2.4 Laminated Pheonolic						
1. Grade 120 laminated Phenolic vs. "R" Monel [15]	Water	0.13	63.8 cc/1000 hour	Smooth Running	1 hour	Thrust-washer wear tester 577 psi, 500 rpm (139 fpm)
2. Grade 124 laminated Phenolic vs. "R" Monel [15]	Water	0.17	22.8 cc/1000 hour	Some Stick-slip	1 hour	Thrust-washer wear tester 577 psi, 500 rpm (139 fpm)
3. Grade 125 laminated Phenolic vs. "R" Monel [15]	Water	0.14	12.5 cc/1000 hour	Smooth Running	1 hour	Thrust-washer wear tester 577 psi, 500 rpm (139 fpm)
4. Grade 112 laminated Phenolic vs. "R" Monel [15]	Water	0.10	12.0 cc/1000 hour	Smooth Running	1 hour	Thrust-washer wear tester 577 psi, 500 rpm (139 fpm)
5. Grade 113 laminated Phenolic vs. "R" Monel [15]	Water	0.10	9.2 cc/1000 hour	Smooth Running	1 hour	Thrust-washer wear tester 577 psi, 500 rpm (139 fpm)
6. Grade 127 laminated Phenolic vs. "R" Monel [15]	Water	0.21	7.7 cc/1000 hour	Smooth Running	1 hour	Thrust-washer wear tester 577 psi, 500 rpm (139 fpm)
7. Grade 127 laminated Phenolic vs. "R" Monel [15]	Synthetic Sea Water		0.100 in.	Quiet	80 hours	Sleeve Bearing operation 577 psi, 15.3 fpm (39 rpm)
3.2.5 Polycarbonate						
1. Polycarbonate vs. "R" Monel [15]	Water	0.042	37.4 cc/1000 hour	Plastic came off in large slivers	1 hour	Thrust-washer wear tester 577 psi, 500 rpm (139 fpm)
2. Glass-filled Polycarbonate vs. "R" Monel [15]	Water	0.067	2.8 cc/1000 hour	Smooth Running,	1 hour	Thrust-washer wear tester 577 psi, 500 rpm (139 fpm)
3. Glass-filled Polycarbonate vs. "R" Monel [15]	Synthetic Sea Water		Excessive	Noisy	80 hours	Sleeve Bearing operation 577 psi, 15.3 fpm (39 rpm)
4. Polycarbonate vs. Inconel 625 [17]	Synthetic Sea Water	0.172	143×10^{-4} cc		1 hour	Thrust-washer wear tester 577 psi, 500 rpm (139 fpm)
5. Polycarbonate vs. Titanium alloy [17]	Synthetic Sea Water	0.25	398×10^{-4} cc		1 hour	Thrust-washer wear tester 577 psi, 500 rpm (139 fpm)

3.2.5 Polycarbonate continued

Test Material Pair	Mode of Lubrication	Coefficient of Friction	Wear Loss	Comments	Test Period	Description of the Test Apparatus
6. Polycarbonate vs. Bronze [18]	Water	0.29	3×10^{-5} in./ft of travel	Swell zero in immersion for 2 months		Continuous sliding test, 52 fpm (100 rpm) 4 lh/in. on 2" φ bearing

3.2.6 Polysulfone

1. Polysulfone vs. "R" Monel [15]	Water		Excessive	Test terminated, 2 minutes	2 min.	Thrust-washer wear tester 577 psi, 500 rpm (139 fpm)
2. Polysulfone vs. Inconel 625 [17]	Synthetic Sea Water	0.173	2.6×10^{-4} cc		1 hour	Thrust-washer wear tester 577 psi, 500 rpm (139 fpm)
3. Polysulfone vs. Titanium [17]	Synthetic Sea Water	0.191	31.2×10^{-4} cc		1 hour	Thrust-washer wear tester 577 psi, 500 rpm (139 fpm)
4. 30% Carbon fiber reinforced Polysulfone vs. 1040 steel [21]	Dry	0.14	75×10^{-10} in.3 min/ft/ lb/hr			Thrust-washer wear tester 40 psi, 50 fpm
5. 30% Glass-fiber reinforced Polysulfone vs. 1040 steel [21]	Dry	0.18	90×10^{-10} in.3 min/ft/ lb/hr			Thrust-washer wear tester 40 psi, 50 fpm

3.2.7 Polyether

1. Chlorinated Polyether vs. "R" Monel [15]	Water	0.076	150×10^{-4} cc	Stick-slip	1 hour	Thrust-washer wear tester 577 psi, 500 rpm (139 fpm)
2. Chlorinated Polyether vs. Inconel 625 [17]	Synthetic Sea Water	0.13	320×10^{-4} cc		1 hour	Thrust-washer wear tester 577 psi, 500 rpm (139 fpm)
3. Chlorinated Polyether vs. Titanium [17]	Synthetic Sea Water	0.18	374×10^{-4} cc		1 hour	Thrust-washer wear tester 577 psi, 500 rpm (139 fpm)
4. Chlorinated Polyether vs. itself [17]	Water	0.16 (13 fpm) 0.09 (52 fpm)	3.58×10^{-5} in./ ft of travel	Swelling in immersion .001 in./in. in 6 months		Continuous sliding operation 52 fpm (100 rpm), 4 lh/in. on 2" φ bearing

3.2.8 Nylon

1. MoS2-filled Nylon vs. "R" Monel [15]	Water	0.12	120×10^{-4} cc	Noisy, violent, stick-slip	1 hour	Thrust-washer wear tester 577 psi, 500 rpm (139 fpm)
2. MoS2-filled Nylon vs. Hastelloy C [17]	Synthetic Sea Water	0.165	202×10^{-4} cc			Thrust-washer wear tester 577 psi, 500 rpm (139 fpm)
3. MoS2-filled Nylon vs. Titanium [17]	Synthetic Sea Water	0.222	24×10^{-4} cc			Thrust-washer wear tester 577 psi, 500 rpm (139 fpm)
4. MoS2-filled Nylon vs. Inconel 625 [17]	Synthetic Sea Water	0.168	4.9×10^{-4} cc			Thrust-washer wear tester 577 psi, 500 rpm (139 fpm)
5. Nylon 6/6 vs. 1040 steel [21]	Dry	0.28	200×10^{-10} in.3 min/ft/lb/hr			Thrust-washer wear tester, 50 fpm, 40 psi
6. 40% carbon fiber reinforced Nylon 6/6 vs. 1040 steel [21]	Dry	0.18	12×10^{-10} in.3 min/ft/lb/hr			Thrust-washer wear tester, 50 fpm, 40 psi

3.2.8 Nylon continued

Test Material Pair	Mode of Lubrication	Coefficient Of Friction	Wear Loss	Comments	Test Period	Description of the Test Apparatus
7. 40% Glass fiber reinforced Nylon 6/6 vs. 1040 steel[21]	Dry	0.21	70×10^{-10} in.^{3} min/ft/lb/hr			Thrust-washer wear tester, 50 fpm, 40 psi
3.2.9 Polyurethane						
1. Polyurethane Coating vs. Bronze[18]	Water	0.40	0.16×10^{-5} in./ft travel	Coating peeled in immersion for 6 months		Continuous sliding, 52 fpm (100 rpm), 4 lb/in on 2"φ bearing
2. Polyurethane Coating (E-143) vs. Bronze[18]	Water	0.28	1.6×10^{-5} in./ft. travel	Swell in immersion .008 in./in. in 6 months		Continuous sliding, 52 fpm (100 rpm), 4 lb/in. on 2"φ bearing
3. Polyurethane (E-130) vs. Bronze[18]	Water	.43	$.67 \times 10^{-5}$ in./ft travel	Swell in immersion .007 in./in. in 6 months		Continuous sliding, 52 fpm (100 rpm), 4 lb/in. on 2"φ bearing
3.2.10 Acetal						
1. Polyacetal vs. Inconel 625[17]	Synthetic Sea Water	0.17	40×10^{-4} cc		1 hour	Thrust-washer wear tester 577 psi, 500 rpm (139 fpm)
2. Polyacetal vs. Hastelloy C[17]	Synthetic Sea Water	0.117	26×10^{-4} cc		1 hour	Thrust-washer wear tester 577 psi, 500 rpm (139 fpm)
3. Polyacetal vs. Titanium[18]	Synthetic Sea Water	0.186	15×10^{-4} cc		1 hour	Thrust-washer wear tester 577 psi, 500 rpm (139 fpm)
4. Acetal + MoS$_2$ vs. Bronze[18]	Water	0.29	3.4×10^{-5} in./ft travel			Continuous sliding test, 52 fpm (1000 rpm) 4 lb/in. on 2"φ bearing
5. Acetal + Teflon fiber vs. Bronze[18]	Water	0.16	4×10^{-5} in./ft travel	Swell in immersion .003 in./in. in 6 months		Continuous sliding test, 52 fpm (1000 rpm) 4 lb/in. on 2"φ bearing
6. Acetal vs. 1040 steel[21]	Dry	0.40	65×10^{-10} in.^{3} min/ft/lb/hr			Thrust-washer wear tester 40 psi, 50 fpm
7. 20% Carbon fiber reinforced Acetal vs. 1040 steel[21]	Dry	0.14	40×10^{-10} in.^{3} min/ft/lb/hr			Thrust-washer wear tester 40 psi, 50 fpm
3.2.11 Buna N Rubber						
1. Buna N rubber vs. Bronze[18]	Water	0.37	0.6×10^{-5} in./ft travel			Continuous sliding test, 52 fpm (100 rpm) 4 lb/in. in 2"φ bearing
3.2.12 Thermoplastic Polyester						
1. 30% Carbon fiber reinforced Polyester vs. 1040 steel[21]	Dry	0.15	24×10^{-10} in.^{3} min/ft/lb/hr			Thrust-washer wear tester, 40 psi, 50 fpm
3.2.13 Polyphenylene Sulfide (PPS)						
1. Polyphenylene Sulphide vs. 1040 steel[21]	Dry	0.24	540×10^{-10} in.^{3} min/ft/lb/hr			Thrust-washer wear tester, 40 psi, 50 fpm

3.2.13 Polyphenylene Sulfide (PPS) continued

Test Material Pair	Mode of Lubrication	Coefficient Of Friction	Wear Loss	Comments	Test Period	Description of the Test Apparatus
2. 30% Carbon fiber reinforced PPS vs. 1040 steel[21]	Dry	0.20	160×10^{-10} in.^{3} min/ft/lb/hr			Thrust-washer wear tester, 40 psi, 50 fpm
3.2.14 Styrene-Acrylonitrile						
1. Styrene-Acrylonitrile vs. 1040 steel[21]	Dry	0.33	$3,000 \times 10^{10}$ in. min/ft/lb/hr			Thrust-washer wear tester, 40 psi, 50 fpm
2. 35% Carbon fiber reinforced Styrene-Acrylonitrile vs. 1040 steel[21]	Dry	0.15	40×10^{-10} in.^{3} min/ft/lb/hr			Thrust-washer wear tester, 40 psi, 50 fpm
3.2.15 Ferrous Alloys						
1. En58E stainless steel vs. itself[22]	10.5 pH Water	1.0	10^9 cm^3/cm kg			Crossed cylinder wear tester and reciprocating wear tester load 10 lb, 1 fpm
2. En58E stainless steel vs. Inconel[22]	Water	0.9	2×10^{10} cm^3/cm kg 5×10^9 cm^3/cm kg			Reciprocating wear tester Crossed cylinder wear tester
3. En58E stainless steel vs. Nimonic 80A[22]	Water	0.4	10^9 cm^3/cm kg			Crossed cylinder wear tester, load 2 lbs. 1 fpm
4. En58E stainless steel vs. Deloro SF-40 (hard facing .015" on stainless steel)[2]	Water	0.35	8×10^{-10} cm^3/cm kg			Crossed cylinder wear tester, load 2 lbs. 1 fpm
5. En58E stainless steel vs. electroplated chromium[22]	Water	0.30	1.5×10^{-9} cm^3/cm kg			Crossed cylinder wear tester, load 2 lbs. 1 fpm
3.2.16 Non-Ferrous Alloys						
1. High-lead-content copper alloy vs. "R" Monel[15]	Water	0.104	111×10^{-4} cc	Noise, Stick-slip	1 hour	Thrust-washer wear tester, 577 psi, 500 rpm (139 fpm)
2. Solid Tungsten carbide vs. solid Tungsten carbide[23]	Water		Bearing wear 0.0006 in.. Shaft wearmil	Max. load 462 psi	90 hours	Sleeve bearing operation 1000 rpm
3. Al$_2$O$_3$ ceramic vs. WC[23]	Water			Rise in friction at 62 psi	90 hours	Sleeve bearing operation 1000 rpm
4. Stellite SF20 vs. WC[23]	Water			Rise in friction at 31 psi	90 hours	Sleeve bearing operation 1000 rpm
5. 18-8 stainless steel vs. WC[23]	Water			Immediate failure due to high friction Max load	90 hours	Sleeve bearing operation 1000 rpm
6. Colmonoy vs. Beryllium Copper[23]	Water			Seizure 46 psi	90 hours	Sleeve bearing operation 1000 rpm
7. Al$_2$O$_3$ ceramic vs. WC[23]	Water			High friction shaft and bearing scored Max load 46 psi	90 hours	Sleeve bearing operation 1000 rpm
8. WC vs. Beryllium Copper[23]	Water		Shaft failure nil. bearing wear-.0004 in.	No failure Max load 462 psi	90 hours	Sleeve bearing operation 1000 rpm

3.2.16 Non-Ferrous Alloys continued

Test Material Pair	Mode of Lubrication	Coefficient Of Friction	Wear Loss	Comments	Test Period	Description of the Test Apparatus
9. High Purity Alumina vs. TiO$_2$ plasma sprayed on 17-4 pH stainless steel[24]	Sea Water			Successfully operated at 3 gpm	500 hrs.	Sea-water pump, 4500 psi
10. Chrome Plate vs. Carbon Graphite P658 RCH[26]	Sea Water	0.0084	5 x 10^{-5} in.	Surfaces Smooth After Test	0.6 hrs.	Thrust-washer wear tester 300 fpm (1000 rpm), 1500 psi
11. Chrome Plate vs. Berylco 50[26]	Sea Water	0.0033	1 x 10^{-5}	Surfaces Smooth After Test	0.6 hrs	Thrust-washer wear tester 300 fpm (1000 rpm), 2000 psi
12. Chrome Plate vs. Colmonoy 4[26]	Sea Water	0.0084	1 x 10^{-5} in.	Surfaces Smooth After Test	0.5 hrs	Thrust-washer wear tester 300 fpm (1000 rpm), 1000 psi
13. Tungsten Carbide K-602 vs. Linde Flame plate LW-526	Sea Water	0.002	Negligible	Surfaces Smooth After Test	1 hr	Thrust-washer wear tester 300 fpm (1000 rpm), 2500 psi
14. Chrome Plate vs. Haynes Stellite 6B[26]	Sea Water	0.0025	2 x 10^{-4} in.	Surfaces Very Rough After Test	6 min	Thrust-washer wear tester 300 fpm (1000 rpm), 1000 psi
15. Chrome Plate vs. Carbon Graphite CCP72[26]	Sea Water	0.0121	7 x 10^{-5} in.	Surfaces Rough After Test	0.6 hrs	Thrust-washer wear tester 300 fpm (1000 rpm), 1000 psi
16. Cemented Tungsten Carbide vs. Cold pressed Al$_2$O$_3$[27]	Nitrogen gas		1.3 x 10^{-3} in.	Test temperature 250°F	45 hrs.	Pin on a flat disc reciprocating wear tester 450 fpm, 1000 psi
17. Cemented Tungsten Carbide vs. itself[27]	Nitrogen gas		6 x 10^{-4} in.	Test temperature 250°F polished surfaces	7 hrs	Pin on a flat disc reciprocating wear tester 450 fpm, 1000 psi
18. Boron Carbide[28,29] vs. Tungsten Carbide vs. Tantalum Carbide vs. Co/Cr/W/Mo alloy	Water		Acceptable			Bearing - 200 psi and 600 fpm
19. WC vs. WC[28]	Water		Acceptable			Bearing - 3900 psi and 4 fpm
20. Co/Cr/W/Mo alloy vs. itself[28]	Water		Acceptable			Bearing - 3900 psi and 4 fpm

TABLE 3.3
MECHANICAL PROPERTIES OF PLASTICS

S. No.	Designation	Density lb/cu. in.	Tensile strength, ksi	Compressive strength, ksi	Flexural strength, ksi	Tensile modulus, psi	Thermal Conductivity, Btu,ft/ hr ft2°F	Coeff. Thermal Expansion /°Fx10^-5	Hardness	Heat Deformation temperature °F	Water Absorption 24 hours %	Dry PV limit psi fpm
1	Noryl GFN3 (30% glass filled) General Electric, Selkirk, N.Y.	0.047	17	17.9	20	1.2×10^6	0.092	1.4	Rockwell L108	300 @ 264 psi	0.06	
2	Polyimide, 15% Graphite filled PI-115 fluorocarbon Tribol Industries Division Santa Ana, California		10.5	20.8	13.7	2.6×10^5 comp.mod. 2.71×10^5				550		
3	Polyimide (thermoplastic) Tribol Industries	0.051	17.1	29.9		1.88×10^5	0.29	2.8				25,000
4	Ekkcel CL 1340 (thermoset linear aromatic polyester), 20% graphite filled Carborundum, Buffalo	0.053	8.5	12.5	7	2.92×10^5 comp.mod. 2.09×10^5	0.58	4.4	E-30	610	0.07	>70,000
5	Ekkcel VR-25 (linear aromatic polyester) Carborundum, Buffalo	0.067	1.8	1.5		compressive modulus 1.4×10^5	0.36	4.2	Shore D 63	600		15,000
6	Porous bronze impregnated with PTFE-Pb mixture with thin overlay of PTFE and Pb (DU Bearing) Garlock Bearing Thorofare, N.J.			yield in compression 44			24 normal to surface	1.7 normal to surface		536		50,000
7	Ryton R-4, 40% glass (thermoplastic polyphenylene sulfide) Phillips, Bartlesville	0.058	19.5	21	29	Flex. mod. 1.7×10^6	.166	1.2	R123	500F @ 264 psi	.05	
8	TORLON 4301 Thermoplastic (Polyamide-imide with fillers) Amoco, Chicago	0.05	19.6	30	26.4	comp.mod. 6.8×10^5 flexural mod. 9.19×10^5	0.21	1.5	M109	525F	0.22	
9	CL-100 cross-linked Polyethylene Phillips Chemical Company, Bartlesville	0.034	2.6			Flex. mod. 10^5		9.22	D61 (shore)	140F @ 66 psi 101F @ 264 psi		
10	Cadco HMW 1900 ultra high molecular weight, high density polyethylene (2 to 5×10^6 MW) Cadillac Plastic and Chemical Company, Albany	0.033	2.5	2.4	1	1.02×10^5	0.283	4	R50	250F continuous exposure		
11	High density Polyethylene Cadillac Plastic	0.034	3.1 to 5.5	2.4	1	$0.8-1.5 \times 10^5$	0.283	6.66	D60-D70 (shore)	160 @ 66 psi	<0.01	
12	Polyimide, 30% PTFE Meldin P130X Dixon Corp., Bristol, Rhode Island	0.057	3.3	13	5.4	comp.mod. 2.8×10^5		3.7	D55			
13	UHMW Polyethylene, 50% bronze powder filled West Lake, Lenmic, Pennsylvania											

TABLE 3.4

MECHANICAL PROPERTIES OF METALS

S. No.	Alloy	Corrosion Resistance	Density lb/cu. in.	Mod. of Elas. x10⁶ psi	Thermal Conduc. Btu/sqft/hr/°F/ft	Coeff. of thermal exp. in./in./°F	Hardness Rockwell	Yield strength ksi	Type of Heat Treatment
1	17-4 PH H-1150, H-900	Pitting occurs	0.284	28.5	10.3	6.6	33 -44 R_C	125 185	Precipation hardenable
2	Nitronic 60 annealed 70% cold drawn	Very good	0.277	26.2		8.8	96 R_B 46 R_C	60 217	Cold drawing, good anti-galling properties
3	Nitronic 50 annealed 46% cold reduction	Exc.	0.285	28	9	9	91 R_B 36 R_C	57 183	Cold drawing
4	NP35-N annealed 53% cold worked	Exc.	0.304	34	6.5	7.1	8 R_C 50 R_C	60 205	Cold drawing
5	Titanium 6 Al-4V	Exc.	0.16	16	4	4.9	30 R_C	120	Precipation hardenable
6	Waukesha 88 Casting	Exc.	0.31	27	16.7	8	15 R_C	38	
7	INCO 625 as rolled	Exc.	0.305	30	5.7	7.1	26 R_C	60-110	Cold drawing
8	C715 annealed 40% cold worked	Exc.	0.323	22	17	9	35 R_B 80 R_B	21 70	Cold drawing
9	Berylco 25 hardened	Exc.	0.298	18.5	62 to 75	9.4	36-41 R_C	145-175	Precipitation hardenable
10	MONEL 403 annealed cold drawn	Very good	0.32	25.2	15	7.7	60-80 R_B 70-100R_B	23-40 45-100	Cold drawing
11	Stellite 6B casting or wrought	Exc.	0.303	31.1	8.58	7.7	39-45 R_C	92.6	Cold drawing
12	440C annealed Hardened	Pitting occurs worse than 17-4 pH	0.28	29	14	5.6	97 R_B 57-60 R_C	65 275	Heat treatable
13	Hastelloy C annealed Hardened	Exc.	0.323	28.5	6.5	7.02	12-19 ? 35 to c 40 R_C	45 to 48 97	Precipation hardenable can be cast
14	Colmonoy 4	Exc.	0.28	32	8.66	6.7			Not heat treatable
15	Colmonoy 70	Exc.	0.28	32	8.66	6.7			Not heat treatable

TABLE 3.5

CHEMICAL COMPOSITION OF METALS

S. No.	Alloy Designation	Ni	Co	Cu	Cr	Mo	Al	V	Fe	Ti	C	Mn	Si	P	S	Other
1	MP35-N	33 to 37	Balance		19 to 21				1	1	.025	.15	.15	.015	.01	
2	Ti 6Al-4V						5.75 to 6.75	3.5 to 4.5	.25	Balance	.08					.05 N
3	Waukesha-88	Balance			11 to 14	2 to 3.5			2		.05	1.25	.5			3 to 5 Sn, 3 to 5 Bi
4	INCO 625	Balance	1.0		20 to 23	8 to 10	.4		5	.4	.1	.5	.5	.015	.015	3.5 Cb
5	Copper Alloy C715	29 to 33		Balance					.4 to 7			1.0				1.0 Zn
6	Berylco 25 CA-172	0.2 Co or Ni	0.6 Co, Ni and Fe	99.5												1.8 to 2 Re
7	Monel 403	55 to 60		Balance					1.0		.3	1.25 to 2.25	.75		.024	
8	Stellite 6B	3	52.9		30						1.1	2	2			4.5 W
9	17-4 PH	3 to 5	15.5 to 17.50	3 to 5		1.5			3		.07					
10	440 C				16 to 18				Balance		.95 to 1.2					
11	Hastelloy C	Balance			15.5 to 17.5	16 to 18		.2 to .4	4.5 to 7		.15	1.0	1.0	.04	.03	3.75 to 5.25 W
12	Colmonoy 4	Balance			10				2.25		.45		2.25			2 B
13	Colmonoy 70	Balance		11.5					3.75		.5		3.25			16 W, 2.5 B

TABLE 3.6

MECHANICAL AND THERMAL PROPERTIES OF OTHER MATERIALS

S. No.	Designation	Density lb/cu. in.	Tensile strength ksi	Comp. strength ksi	Flexural strength (transverse) ksi	Mod. of Elasticity x10^6 psi	Thermal conductivity Btu/sq ft/hr/°F/ft	Coeff. of thermal exp.x10^{-6} in./in./°F	Hardness	Comments
1	Ferrotic HT-2 annealed hardened Chromalloy, W. Nyack, NY	0.23				42		5.3	R$_c$ 44 R$_c$ 54	Age hardenable Nickel-Iron matrix. Good machinability.
2	Purebon Carbon Graphite P-658 RCH Pure Carbon, St. Marys, PA	0.065	6.5	31	9	3.3	5	2.6	95 Scleroscope C	PV limit 1.7 x 10^6 psi, fpm
3	NEDOX General Magnaplate Linden, NJ	Controlled infusion of PTFE within hard nickel alloy plating of electroless nickel.							R$_c$ 65	Coating thickness, 0.0002-0.003 in.
4	High purity (99.5%) Al$_2$O$_3$ AD-995 Coors Porcelain, Golden, Co.	0.14	38	380	55	54	20.57	1.88	83 Rockwell R45 N	
5	Silicon Carbide Densified (KT)	0.112	15	150	24	55	25 (1832°F)	2.17		Max. use temperature 3000°F
6	Titanium Carbide hot pressed or steel die pressed and sintered.	0.21-0.22	26-134	420-520	125-200	57.5-66	9.9-13.1 (212°F)	4.4-4.6 (68 to 1200°F)	A89-A93.5	
7	Tungsten Carbide (WC) Kennametal	.38-.55	130 (75°F)	400-820	120-400	64.5-101	16.4-68.9 (212°F)	2.2-4.1 (68°F to 1200°F)	A83.5-94.3	
8	Silicon Nitride	.111				45	0.9 (400-1200°F)	1.37	A99	
9	Alumina-Titania composite (plasma sprayed)	Physical combination of alumina and 13 wt% titania							K$_c$ 65-70	Coating thickness, about 0.003 in.

for many alloys when coupled to them in sea water. Therefore, although some of these materials have very desirable friction, wear, erosion, and corrosion characteristics, it was decided that they should be avoided if possible. To reduce the probability of galvanic corrosion, it was desirable that the number of alloys used in the motor be minimized and/or that those used should be galvanically compatible in sea water.

Molybdenum disulphide react with water and oxygen in the air available and form sulphuric acid which is undesirable. Therefore, plastics with MoS_2 fillers, though good in minimizing wear, should be avoided.

Some of the criteria used in the study for the selection of materials were as follows:

- High corrosion resistance in sea water.
  General corrosion and pitting, crevice corrosion, and galvanic corrosion.

- Good mechanical strength (bending stress and compressive stress) to support load, and high hardness to reduce abrasive wear.

- High thermal conductivity to dissipate heat generated at the interface.

- Low thermal expansion to avoid distortion due to local heating.

- Low static and kinetic friction to minimize power losses.

- Low wear rate.

- High heat deformation temperature and low swelling in water submersion in case of plastics.

- Good anti-galling properties for metal-metal combinations.

- Good availability.

- Good machinability.

- Low cost.

The selected material combinations have been divided into three categories.

3.3.2 Plastic-Metal Combinations

The analyses conducted to establish the operating condition of the motor (Table 2.14) showed that the bending and compressive strengths and the PV (pressure x velocity) limit of plastics, if used, should be high to withstand forces to be exerted in some critical areas of a motor. Based on mechanical properties and prior experience, several plastic candidates were recommended and are listed in Table 3.7. Since the list of the viable candidates was very long, only materials with first priority were selected for tests.

Wear tests conducted by Thomas and Halliwell [17] to study the compatibility of plastics with metallic members in water showed that the wear of a plastic member may vary much depending on the mating metallic member. In their study,

TABLE 3.7

SELECTED PLASTIC MATERIALS

First Priority

1. Polyethylene, ultra high molecular weight (UMHW)

2. Noryl, 30 percent glass filled

3. DU bearing material (porous bronze impregnated with PTFE-Pb mixture with thin overlay of PTFF and Pb)

4. Polyethylene, UHMW, 50 percent bronze powder filled.

5. Polyimide, 30 percent PTFE filled.

6. Torlon 4301 (Polyamide - imide with fillers)

Second Priority

7. Polyethylene, cross-linked.

8. Polyethylene, high density, 5 percent graphite fiber filled.

9. Polyethylene, high density, 15 percent Cu and 10 percent Pb filled.

10. Polyethylene, high density, 10 percent SiC, 15 percent PTFE filled.

11. Polyethylene, high density, 30 percent Kaolin filled.

12. Polyimide, 15 percent graphite and 10 percent PTFE filled.

13. Polyimide, 20 percent Kevlar aramid - reinforced.

14. Phenolic, 15 percent graphite filled.

15. Acetal, 30 percent PTFE filled.

16. Ryton (polyphenylene sulphide) with TFE and glass filled.

17. Ryton with graphite.

18. Slip liner (bronze wire mesh in teflon and other constituents).

19. Ekkcel (linear aromatic polyester).

metallic members selected were Titanium-6Al-4V, Hastelloy C, Inco 625, and "R" Monel. Their results showed that Inco 625 running against plastics, in general, had lower wear. A study to select the most corrosion-resistant ball valve material in sea water service (Reference 30) concluded that among Monel, 70-30 Cu-Ni, Hastelloy C, Inco 625, 304 Stainless, and Ti 6-4 materials tested, Ti 6-4 looked most promising based on sea water corrosion data. However, it was believed that Ti 6-4 is not a good anti-galling material.

Data supplied by Kawecki-Berylco Industries, manufacturer of Be-copper alloys indicate that their alloys are good in wear application only if they are properly lubricated. Therefore, it was felt that they may not be very good in sea water-lubricated conditions. MP35-N may be good in wear due to high cobalt content. 440C is a good bearing material but its long-term corrosion in sea water is not as good as other materials. Nitronic 50 is excellent in corrosion. Since it is relatively cheap and easier to machine, it was thought to be a good candidate.

The following metallic alloys were selected to be run against plastics.

- Nitronic 50

- Inco 625

- MP35-N

All the plastics were first tested against Nitronic 50. The plastics from the best combinations were then tested against Inco 625 and subsequently against MP35-N. By this technique, the best plastic-metal combination could be found. The recommended plastic-metal combinations are listed in Table 3.8.

3.3.3 Metal-Metal Combinations

Leaded tin bronze (SAE 660) - 440C combination was selected to provide a baseline reference for metal-metal combinations.

One of the critical requirements of materials in this category is that they should have good anti-galling properties. Some work at Armco has shown that as long as one of the members has good anti-galling properties, the combination is usually satisfactory. Both Waukesha 88 and Nitronic 60 were believed to have excellent anti-galling properties (Reference 32) and Nitronic 50 also has acceptable anti-galling properties. Therefore, most of the combinations were made with either Waukesha 88, Nitronic 60, or Nitronic 50. Due to its high cobalt content, MP35-N was thought to be a good candidate and was used. The materials 440C and Stellite 6B are good sliding members. The selected combinations are presented in Table 3.9.

3.3.4 Other Nonmetal-Metal Combinations

In the design of a high-pressure sea water piston type pump [24], the cylinders within which the pistons reciprocate were made of high purity alumina ceramic. The pistons were 17-4 PH stainless steel, plasma sprayed with titanium dioxide. It is found that plasma sprayed coatings exhibited microscopic porosity; consequently, in corrosive environments, there is a danger of corrosive agents penetrating through the microscopic pores to the substrate. A coating of Alumina-Titania (13 wt % TiO_2 and remaining Al_2O_3), when plasma sprayed, deposits as an unusually dense structure (Reference 33) which is practically immune to

TABLE 3.8

PLASTIC-METAL COMBINATIONS FOR SCREENING TESTS

S. No.	Plastic vs.	Metal	Continuous Wear Test	Reciprocating Wear Test
1	Polyethylene, ultra high molecular weight	Nitronic 50	X	X
2	Noryl GFN-3, 30% glass filled	Nitronic 50	X	X
3	DU bearing material	Nitronic 50	X	
4	UHMW Polyethylene, 50% bronze powder	Nitronic 50	X	X
5	Polyimide, 30% PTFE	Nitronic 50	X	X
6	Polyamide-imide with fillers (Torlon 4301)	Nitronic 50	X	X
7		INCO 625	X	X
8	Best Three Plastics	INCO 625	X	X
9		INCO 625	X	X
10	Best two (in 1,2,4,5,&6)	MP35N	X	
11		MP35N	X	

TABLE 3.9

METAL-METAL COMBINATIONS FOR SCREENING TESTS

S. No.	Metal vs.	Metal	Continuous Wear Test	Reciprocating Wear Test
1	440C	Leaded tin bronze (baseline)	X	X
2	Waukesha 88	MP35N	X	
3	Nitronic 50	MP35N	X	
4	440C	440C	X	X
5	Waukesha 88	Waukesha 88		X
6	Waukesha 88	Nitronic 50		X
7	Waukesha 88	INCO 625		X
8	Nitronic 50	INCO 625		X
9	Nitronic 50	Nitronic 60		X
10	Stellite 6B	Stellite 6B		X
11	NEDOX plating* on Nitronic 50	NEDOX plating* on Nitronic 50		X

* Controlled infusion of PTFE within hard nickel alloy plating of electroless nickel

submersion in sea water. The combination of solid high purity Al_2O_3 (AD-995, Coors Porcelain Company) and plasma sprayed Alumina-Titania was selected for tests. Another coating, Kaman SCA,consisting of an alumina-chromia composite ceramic material which is a proprietary coating of Kaman Sciences Corp., Colorado Springs,was believed to have good wear properties in a marginally lubricated condition and was selected for tests.

Ferro-TiC HT-2 is a dispersion of extremely hard titanium carbide grains in a heat-resistant, nickel-chromium-iron age-hardenable alloy matrix. It was claimed by the manufacturer, Chromalloy American Corporation, that this material exhibits good strength and resistance to oxidation, corrosion, and wear. It can be machined in solution-annealed condition, and then hardened by an aging treatment to R_c54 and was selected for tests.

Reciprocating wear tests on hard-hard combinations were conducted in Freon environments by Murray and Peterson [27] and their study concluded that alumina against tungsten carbide had the least wear. Graphite is a known good sliding member. As mentioned earlier, although graphite is not good in sea water from a corrosion standpoint, it was selected to provide a back-up in case other combinations did not perform satisfactorily. Graphite was tested against chrome plated Nitronic 50. The selected material combinations are listed in Table 3.10.

3.4 Matching of Materials with Critical Component Requirement

Loading and speed conditions of critical components in each motor type were calculated in Chapter 2. Based on the material requirements and mechanical and tribological properties of the potential material combinations, the material combinations were selected for critical components in each motor type. The selections for gear, vane, and piston type motors are tabulated in Tables 3.11 through 3.13.

TABLE 3.10

OTHER NONMETAL-METAL COMBINATIONS FOR SCREENING TESTS

S. No.	Material	Material	Continuous Wear Test	Reciprocating Wear Test
1	Al_2O_3 solid	Alumina-Titania (plasma sprayed, Ni-Cr undercoat) on Nitronic 50 base		X
2	Kaman SCA*	Kaman SCA*		X
3	Ferro-TiC HT-2 (composite)	Ferro TiC HT-2		X
4	Al_2O_3 solid	WC, Plasma sprayed Ni-Cr undercoat on Nitronic 50 base		X
5	Al_2O_3 solid	440C	X	
6	Purebon P 658 RCH	Hard Chrome Plated Nitronic 50	X	X

*Aluminum oxide-chrome oxide composite coating by Kaman Sciences corp, Colorado Springs.

TABLE 3.11

PRELIMINARY SELECTION OF MATERIALS FOR CRITICAL COMPONENTS OF GEAR TYPE MOTOR

Item No.	Name of Part	Materials	
		Case I Metal/Metal External	Case II & III Metal/Plastic External and Internal
1	Shaft	Nitronic 50; Inco 625	Nitronic 50; Inco 625
2	Sleeve Bearing	Insert of any plastic listed in Table 3-8, Item Nos. 1 through 6 or graphite.	Insert of any plastic listed in Table 3-8, Item Nos. 1 through 6 or graphite.
3	Gears	Metal combinations listed in Table 3-9. Item Nos. 4 through 11 and Item No. 3 in Table 3-10.	Metals-Nitronic 50; Inco 625; and MP35N. Plastics-Polyimide with 30 percent PTFE; Torlon 4301; and Noryl GFN3.
4	Thrust Plate	Overlay of any plastic listed in Table 3-8, Item Nos. 1 through 6 and Waukesha 88	Overlay of any plastic listed in Table 3-8, Item Nos. 1 through 6 and Waukesha 88.
5	Housing	MP35N if gears are made of metals and Al_2O_3 sleeve if gears are made of Al_2O_3 and WC.	MP35N if gears are made of metals and Al_2O_3 sleeve if gears are made of Al_2O_3 and WC.

TABLE 3.12

PRELIMINARY SELECTION OF MATERIALS FOR CRITICAL COMPONENTS OF VANE TYPE MOTOR

Item No.	Name of Part	Materials	
		Case I Composite Vane	Case II Hard Vane
1	Shaft	Nitronic 50; Inco 625.	Nitronic 50; Inco 625.
2	Sleeve Bearing	Insert of any plastic listed in Table 3-8, Item Nos. 1 through 6 or graphite.	Insert of any plastic listed in Table 3-8, Item Nos. 1 through 6 or graphite.
3	Vane	Plastic vane tip and remaining made of Nitronic 50 with plastic coating on sides rubbing rotor-plastic listed in Table 3-8, Items 1, 2, 4 to 6.	Waukesha 88; and Plasma sprayed WC on Inco 625 or Nitronic 50 base.
4	Slotted Rotor	Nitronic 50; Inco 625	Waukesha 88; Nitronic 50; and Inco 625 if vane is made of Waukesha 88. Al_2O_3 or faces of Al_2O_3 in the slots and Inco 625 base if vane is made of WC.
5	Outer Ring Track	MP35N	MP35N if vane is Waukesha 88. Al_2O_3 sleeve in MP35N base if vane is WC.
6	Thrust Plate	Overlay of any plastic listed in Table 3-8, Item Nos. 1 through 6	Overlay of any plastic listed in Table 3-8, Item Nos. 1 through 6.

TABLE 3.13

PRELIMINARY SELECTION OF MATERIALS FOR CRITICAL COMPONENTS OF PISTON TYPE MOTOR

Item No.	Name of Part	Material
1	Cam Plate	Nitronic 50; Inco 625; and 440C
2	Slipper	Plastic overlay listed in Table 3-8, Items 1, 2, 4 to 6; and 440C
3	Ball	Nitronic 50; Inco 625; and 440C
4	Piston/Cylinder	Items 1 through 6 listed in Table 3-10.
5	Thrust Plate	Plastic overlay listed in Table 3-8, Items 1 to 6.
6	Sleeve Bearing	Plastic inserts listed in Table 3-8, Items 1 to 6 and graphite
7	Shaft	Nitronic 50; and Inco 625.

4.0 WEAR EXPERIMENTS

Loading and speed (P and V) conditions of critical components of the three motor types were calculated and the selection of material combinations was based on the PV requirements. Limited wear data at certain loading and speed conditions are available on some combinations, but from *that data it may be difficult to* estimate the wear rate under required load x veloctiy (PV) in sea water lubricated conditions. In order to get a fair comparison, it was felt that selected potential material combinations should be tested under identical simulated sliding conditions within the limitations of the program scope and availability of suitable test equipment. Many times the same material combinations were selected for more than one component in the motors and the PV requirements were different for different compcnents. The tests were conducted at the highest PV requirements of each material group so that the tests were accelerated for some component requirements.

The following types of motion occurring in the motors were simulated for the study:

- Continuous sliding

- Reciprocating sliding

- Rolling possibly combined with sliding

A unidirectional continuous sliding tester which utilizes a rotating disc and a stationary loader pin was prepared and used to test the materials to simulate continuous sliding conditions representative of the motions, e.g., in bearings, vane and vane track, slippers, etc.

A reciprocating sliding tester which utilizes a stationary loader plate and a reciprocating pin was prepared and used to test the materials to simulate linear reciprocating sliding motion representative of the motions in piston-cylinder, vane-rotor, etc. The rolling motion on the gear teeth in the gear type motor, ball on a cam track in the piston type motor was also simulated to some degree by this test rig.

4.1 Description of the Tests

4.1.1 Unidirectional Continuous Sliding Tester

The unidirectional sliding test rig was modified from an existing rig for sea water operations. In the test rig, a stationary pin rubs against the circumference of a rotating disc. The pin was loaded by dead weights and the disc was rotated by a variable speed motor. The frictional force was measured by a load cell (Model No. MB-50, manufactured by Interface, Inc., Scotsdale, Arizona). The output of the load cell was fed to a Sanborn chart recorder (Model 321) and continuous trace of the frictional force versus time was obtained. The rate of wear was obtained by measuring the change in the length of the pin with a dial indicator. Assuming that the wear rate remains constant, the wear rate from the test data was calculated for 100 hours. It will be pointed out from the results that the wear rate is initially high and then it drops off considerably. Therefore, the total wear in 100 hours will be less than reported in tables 4.1 through 4.6.

The static frictional force was estimated by rotating the shaft by hand and measuring the force required to move the disc. The disc and the pin were surrounded by a container made of plexiglass which was filled with synthetic sea water. A plexiglass plate was placed below the pin holder to reduce the water pressure which would tend to push the water out of the container.

Since the frictional heat dissipated at the rubbing interface heated up the water, a stainless steel coil was placed in the container and the cold water was circulated through it during the experiment to maintain the water bath temperature close to room temperature. A photograph and a schematic drawing of the test rig are shown in Figures 4.1 and 4.2, respectively.

Due to the low viscosity of sea water, the lubricant film thickness generated at the interface would be in micro-inches. To take advantage of this lubricant film, mating surfaces had to be very smooth and precise, otherwise the film would be lost in deeper valleys. Therefore, all the metallic specimens were ground to 2 rms. The drawings of the disc and pin specimens are shown in Figures 4.3 and 4.4. A photograph of the disc and pin is shown in Figure 4.5.

The rig is capable of operating up to 5,000 rpm (2,600 fpm) and 3,000 psi, i.e., PV of 7.8×10^6 (psi x fpm). The following measurements were made on the test samples in the experiments:

- Length of the pin before and after tests for calculating wear.

- Outer diameter of the disc before and after test for calculating total wear of disc.

- Transverse surface roughness of the disc before and after tests.

- Record of normal load and surface speed.

- Static and dynamic run-out of the disc.

- Change in length of the pin and radius of the disc during experiment with dial indicator every two hours for calculating wear rate.

- Static frictional force.

- Kinetic frictional force versus time during test at interval of every two hours.

- Photographs of the worn surfaces for record.

The static and dynamic run-outs of the discs were controlled to 0.0003 inch. All specimens due to the geometry of a flat surface rubbing on cylindrical surface started with a line contact and, as the specimens wore, the contact area increased with a consequent reduction in the stress. Theoretically, the stress at the interface at starting could be very high. To minimize the possibility of any catastrophic failures at starting, the specimens were run in at very low load (pan alone = 1.4 lbs) and low speed (1500 rpm) for fifteen minutes. Then the load and speed were slowly increased to the test conditions. The tests were run until the pin wore a detectable amount (0.5-5 mils) or the friction increased considerably.
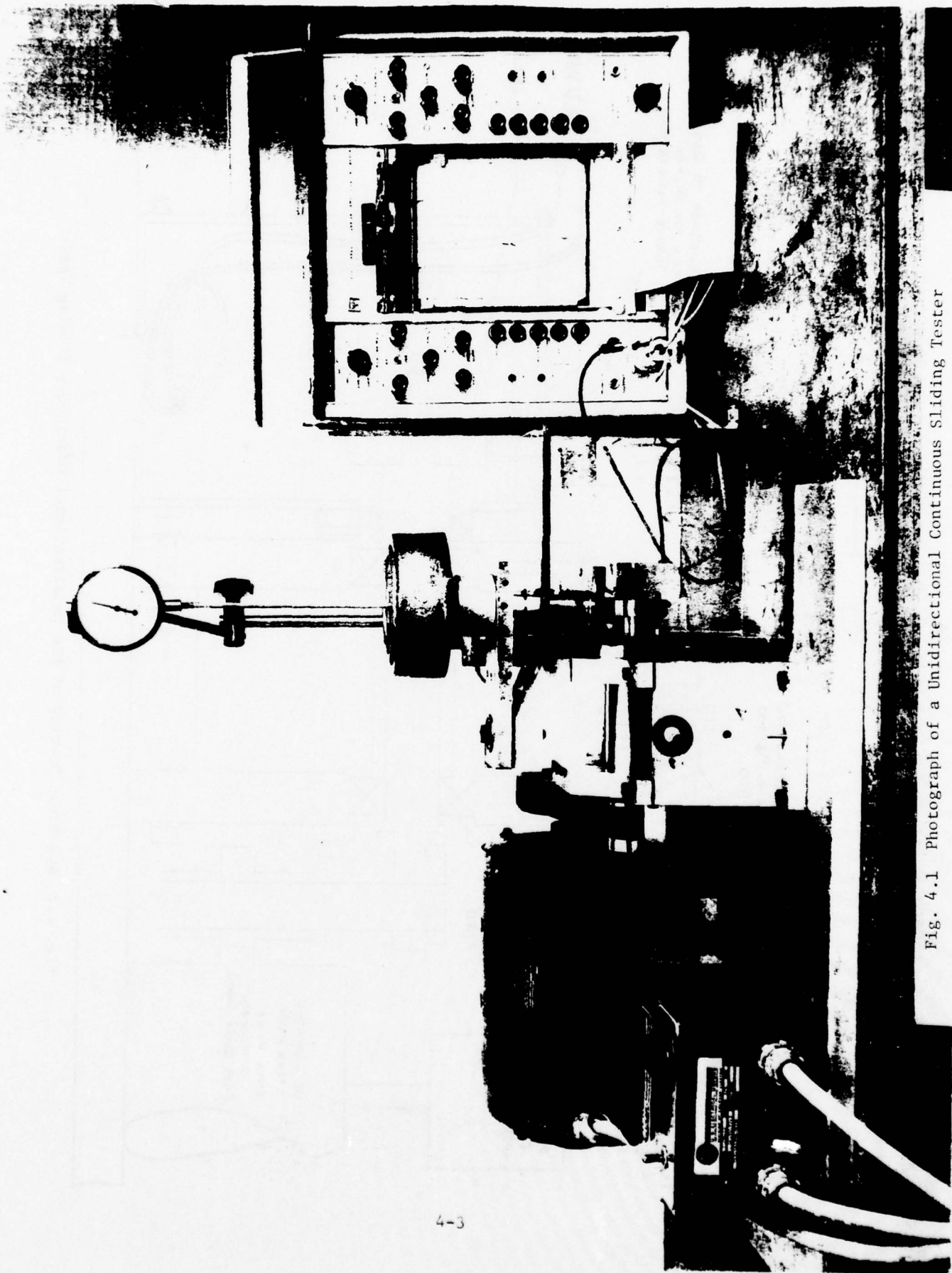
Fig. 4.1 Photograph of a Unidirectional Continuous Sliding Tester

4-3
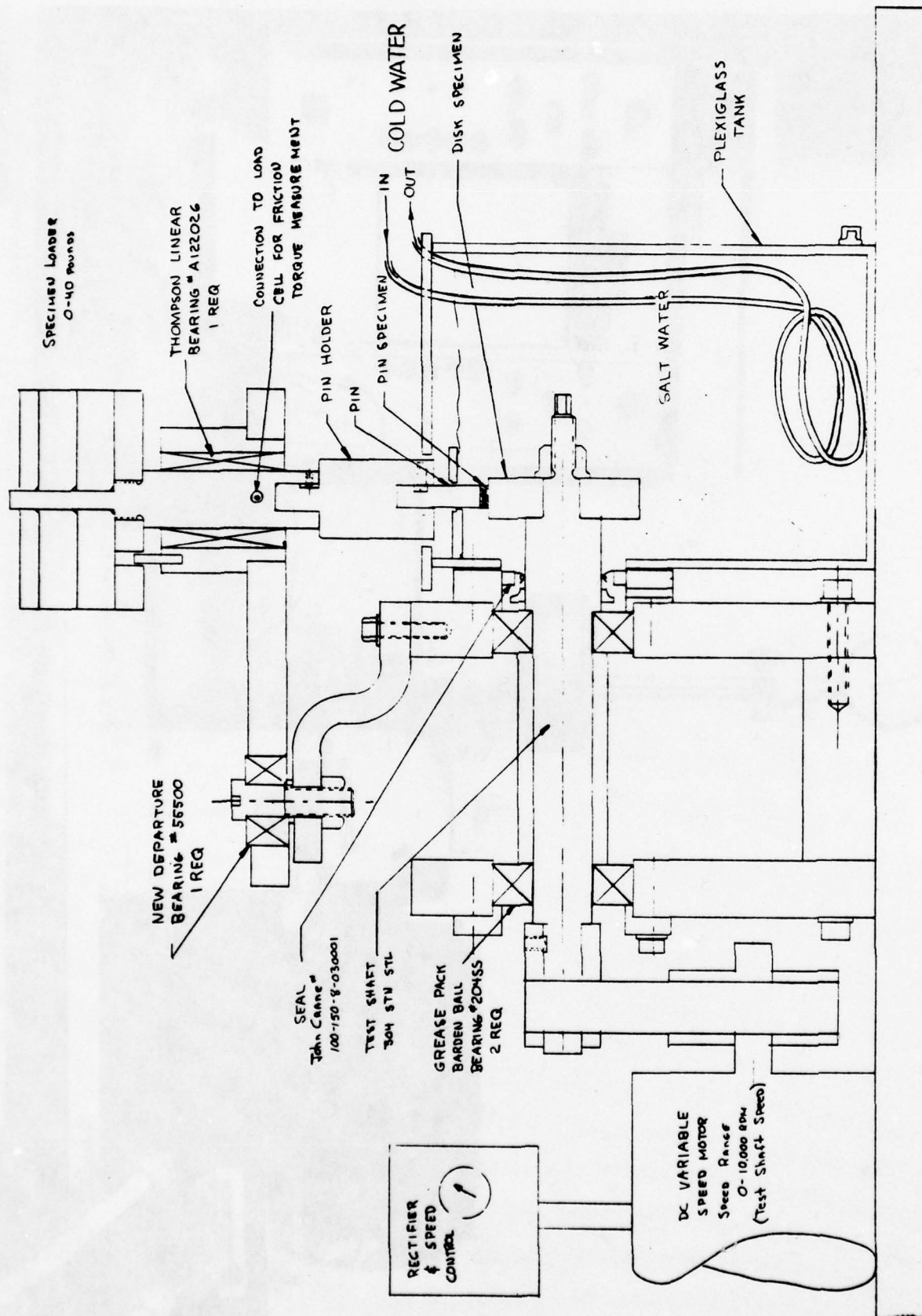
Fig. 4.2 Schematic Drawing of the Unidirectional Continuous Sliding Tester

SPECIMEN LOADER
0-40 POUNDS

THOMPSON LINEAR
BEARING # A122026
1 REQ

CONNECTION TO LOAD
CELL FOR FRICTION
TORQUE MEASUREMENT

PIN HOLDER

PIN

PIN SPECIMEN

IN

OUT

COLD WATER

DISK SPECIMEN

SALT WATER

PLEXIGLASS
TANK

NEW DEPARTURE
BEARING # 56500
1 REQ

SEAL
John Crane #
100-150-8-030001

TEST SHAFT
304 STN STL

GREASE PACK
BARDEN BALL
BEARING #204SS
2 REQ

RECTIFIER
& SPEED
CONTROL

DC VARIABLE
SPEED MOTOR
SPEED RANGE
0-10,000 RPM
(TEST SHAFT SPEED)
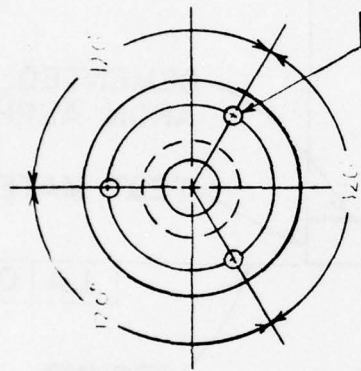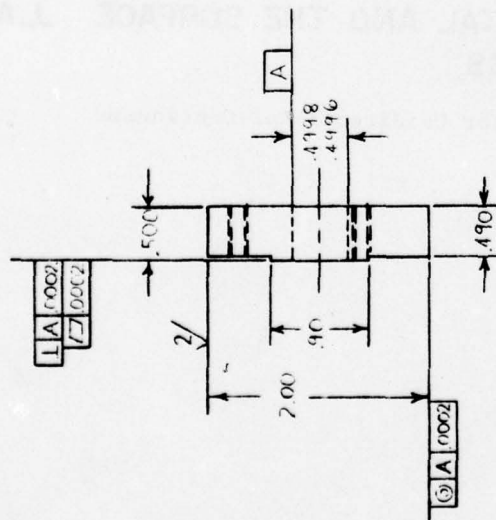
Fig. 4.3 Sketch of the Disc for Unidirectional Sliding Tester
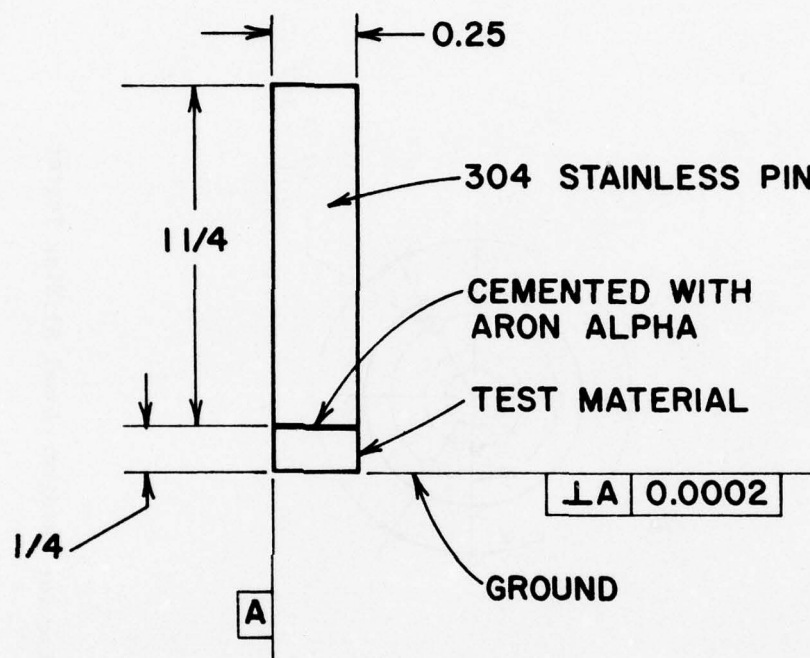
NOTE: METALLIC TEST SPECIMENS WERE MADE ENTIRELY
OF THE TEST METAL AND THE SURFACE ⊥A WAS
GROUND TO 2 RMS.

Figure 4.4   Sketch of the Pin for Unidirectional Continuous
Sliding Tester

Fig. 4.5 Photograph of the Test Specimens for Unidirectional
Continuous Sliding Tester

Typically, tests with plastic-metal combinations lasted about thirty hours, while other tests were short (less than one hour).

After a test, the worn area of the pin was measured and from this the final interface stress was estimated.

4.1.2 Reciprocating Sliding Tester

The reciprocating sliding tester was fabricated from standard commercial components. The rig consists of a circular pin rubbing on a plate under load submerged in synthetic sea water. The reciprocating motion was provided by a commercially available sawzaal. The pin was mounted on the reciprocating shaft. The plate was mounted on a hand press. Clear estane bellows, 0.010 inch thick, 1 inch in ID, 1.75 inch OD, with five convolutions with one cough end 1 inch in diamter and 0.5 inch long, and other flange end (made by Gagne Associates, Binghamton, New York), were put over the reciprocating sawzaal shaft exposed to sea water in order to provide a seal to prevent any corrosion of the drive mechanism.

A plexiglass container was put around the specimen assembly to contain synthetic sea water. A hole in the lid of the container was made to release all the pumped air due to extension and compression of the bellows seal. The load at the rubbing interface was provided by loading the lever arm of the hand press.

The wear rates of the pin and plate were determined from measurements with a dial indicator. The photographs and a schematic drawing of the test rig are shown in Figures 4.6 through 4.8. The drawings of the plate and pin are shown in Figures 4.9 and 4.10. A photograph of the disc and pin is shown in Figure 4.11. The test end of the pin was made slightly spherical to prevent any edge contact and grooving.

In calibrating the rig, a load cell was inserted between the plate and the pin. The load was applied on the lever arm, the load acting at the pin-plate interface was measured by the load cell, and a load calibration curve was obtained (Figure 4.12). A capacitance probe was mounted on the reciprocating shaft to measure static and dynamic run-outs. The specimens were loaded, the pin was moved by turning the motor by hand, and static run-out was measured. If the run-out was greater than 0.0002 inch over 3/4 inch stroke, shims were placed under the hand press to obtain the desired run-out. The test rig was put on rubber pads to dampen any vibrations. The dynamic run-out in the loaded condition was less than 0.001 inch. The rig was thoroughly checked for desired accuracy.

The rig is capable of operating up to 1500 psi and 2000 strokes/minute (3/4 inch stroke). The average surface speed is 250 fpm. If the motion is assumed to be sinusoidal:

$$V(t) = V_{max} \sin (\omega t)$$

where V is the velocity, t is the time, and π/ω is the time of the half stroke. V_{max} may be calculated by integrating velocity with time to derive expression between stroke length, ω and V_{max}, and using the definition of average velocity. The expression for V_{max} is:

$$V_{max} = 1.57 \ V_{ave}$$

$$= 1.57 \times 250 = 393 \ \text{fpm}$$
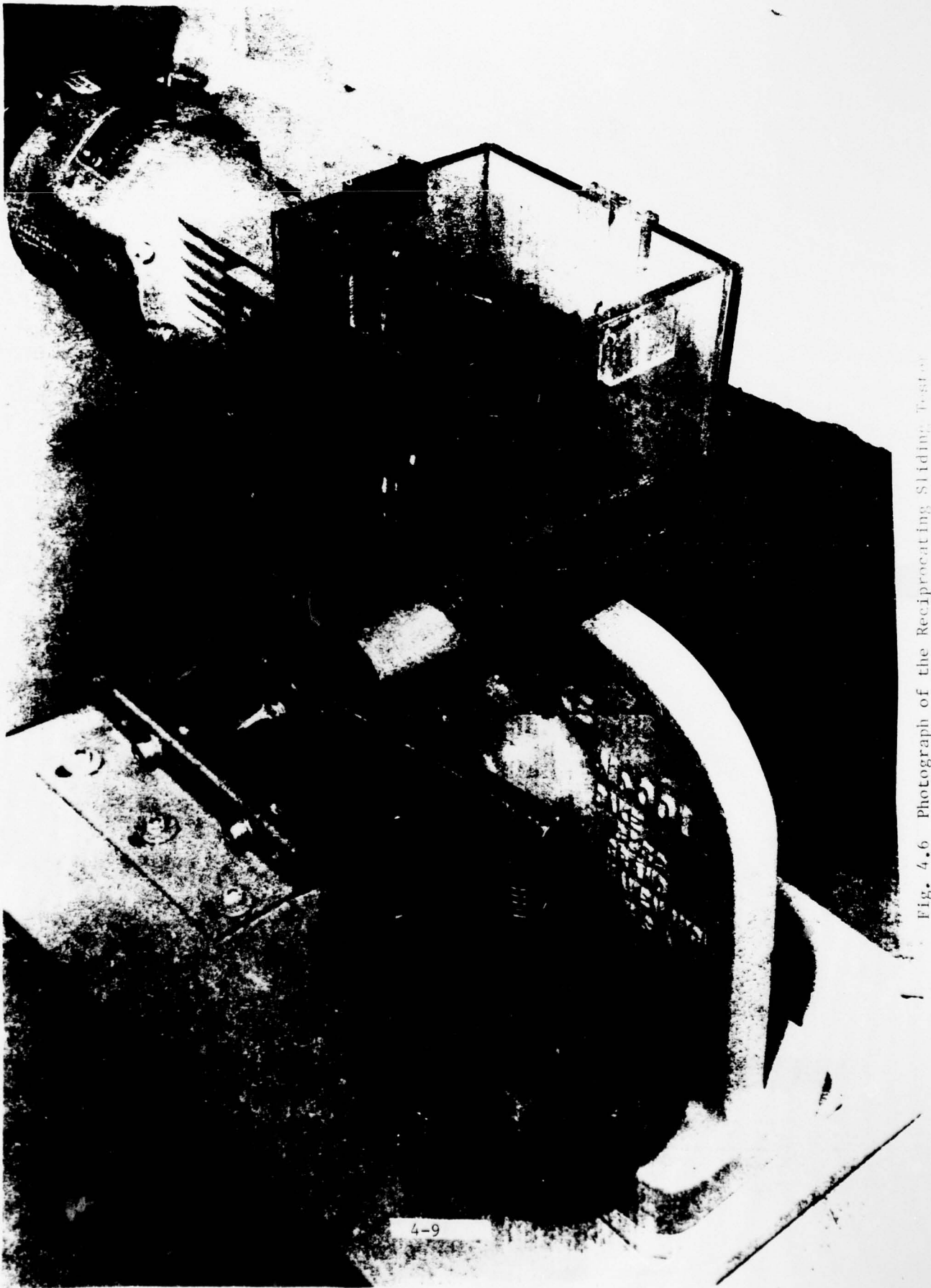
Fig. 4.6 Photograph of the Reciprocating Sliding Tester

4-9

Fig. 4.7 Photograph of the Pin and Plate Specimens in the Reciprocating Sliding Tester

PIN SPECIMEN

PLATE SPECIMEN

PLEXIGLASS TANK

DIAL INDICATOR

PIN

SALT WATER

BELLOWS

MILWAUKEE SAWZALL
#6511 2000/2400 strokes
¾ INCH STROKE

SPECIMEN LOADER
O - 15 lbs.

DAKE NO. 001
HAND PRESS
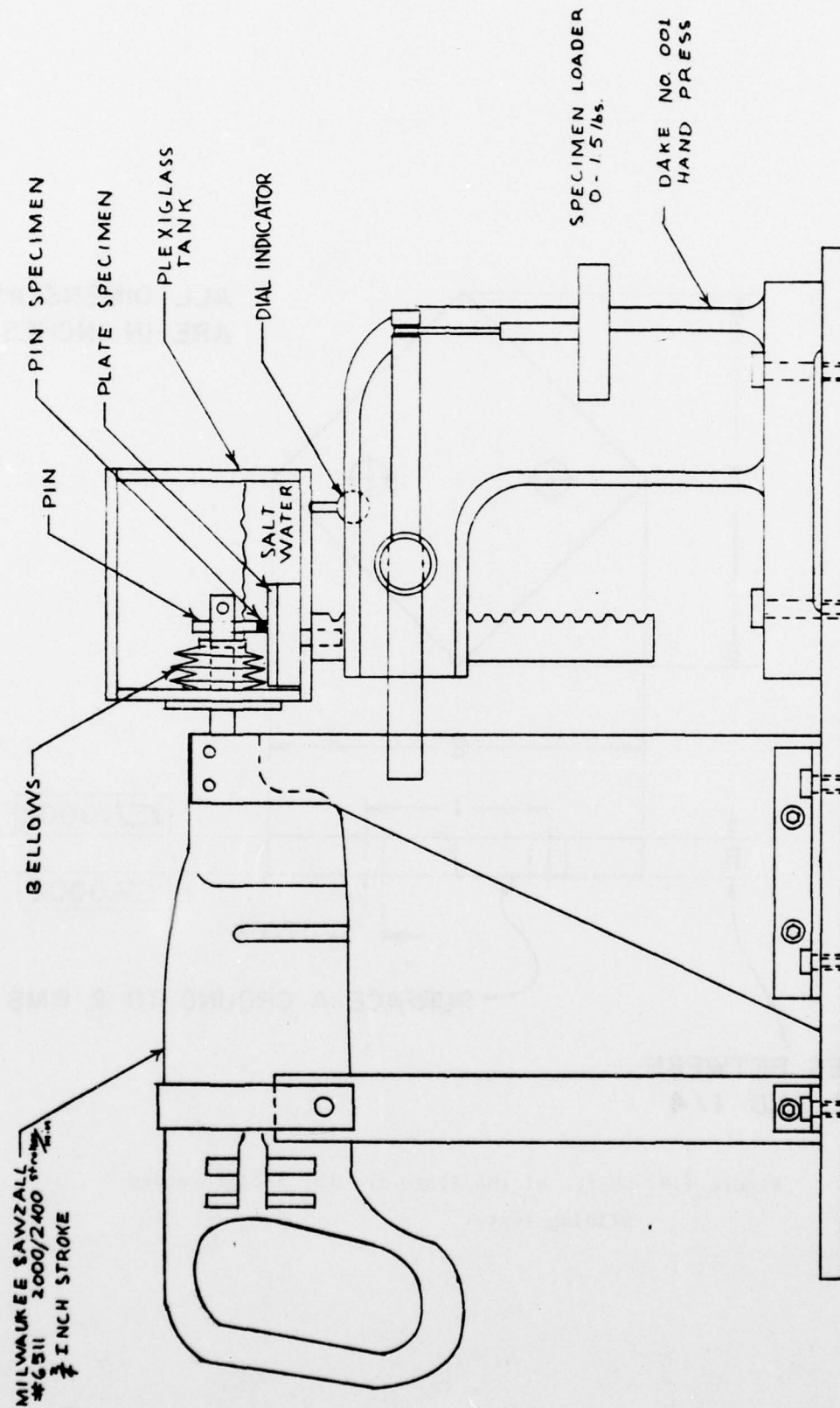
Fig. 4.8 Schematic Drawing of the Reciprocating Sliding Tester

ALL DIMENSIONS
ARE IN INCHES

2

2

1

17/64

B

SURFACE A GROUND TO 2 RMS

B VARIES BETWEEN
1/32 AND 1/4

▱ .0002 | II A .0002

▱ .0002 | -A-
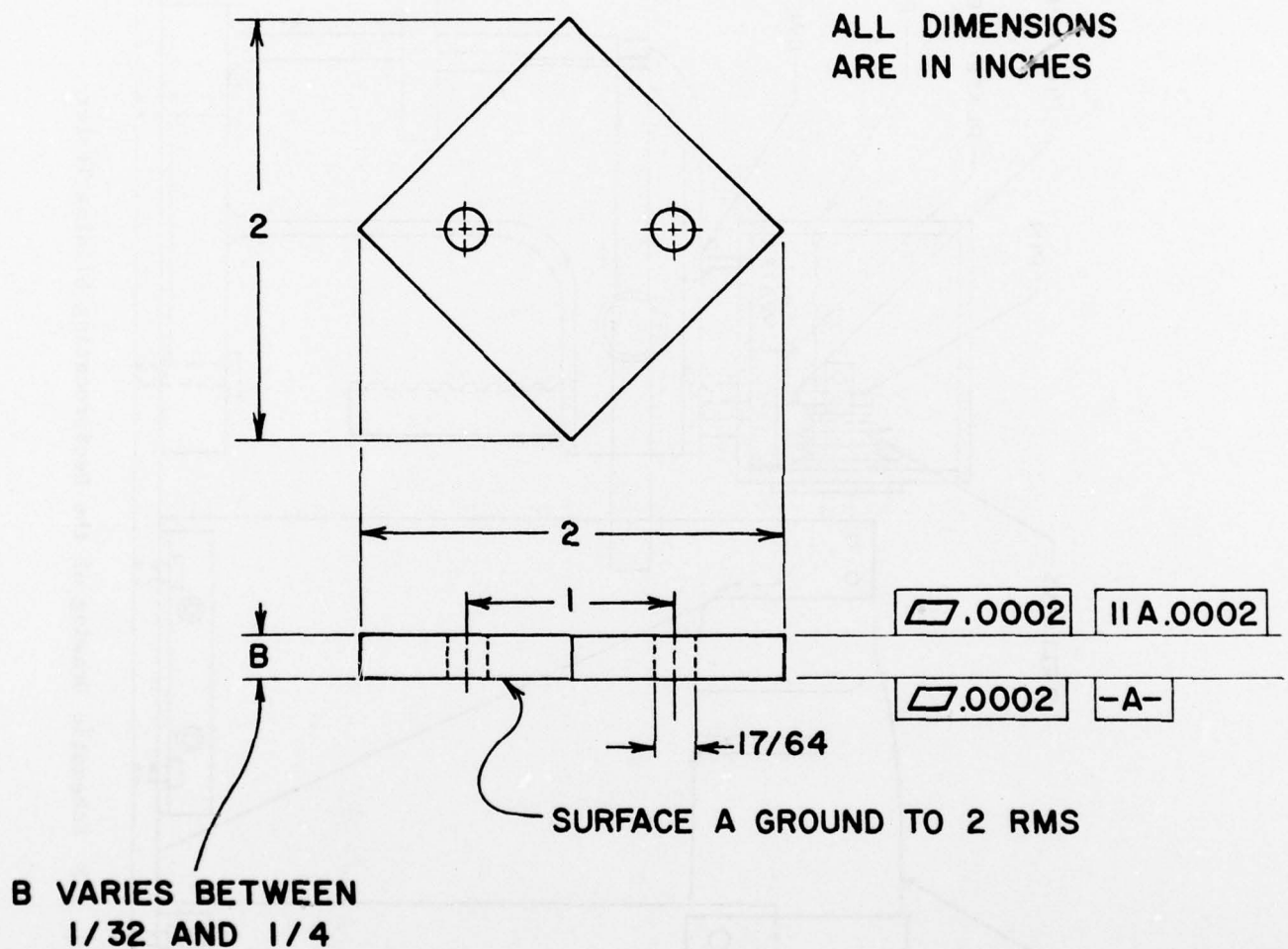
Figure 4.9   Sketch of the Plate for the Reciprocating
Sliding Tester

MTI   MECHANICAL
TECHNOLOGY
INCORPORATED

0.245
0.250

304 STAINLESS PIN

10 INCH SPHERICAL RADIUS

CEMENTED

TEST MATERIAL

1 1/4

1/8

1/8

1/8

ALL DIMENSIONS
ARE IN INCHES

GROUND TO 2 RMS FOR METALS

Figure 4.10   Sketch of the Pin for the Reciprocating
Sliding Tester

MECHANICAL
TECHNOLOGY
INCORPORATED

Fig. 4.11 Photograph of the Test Samples for Reciprocating Slider Tester

MECHANICAL TECHNOLOGY INCOR
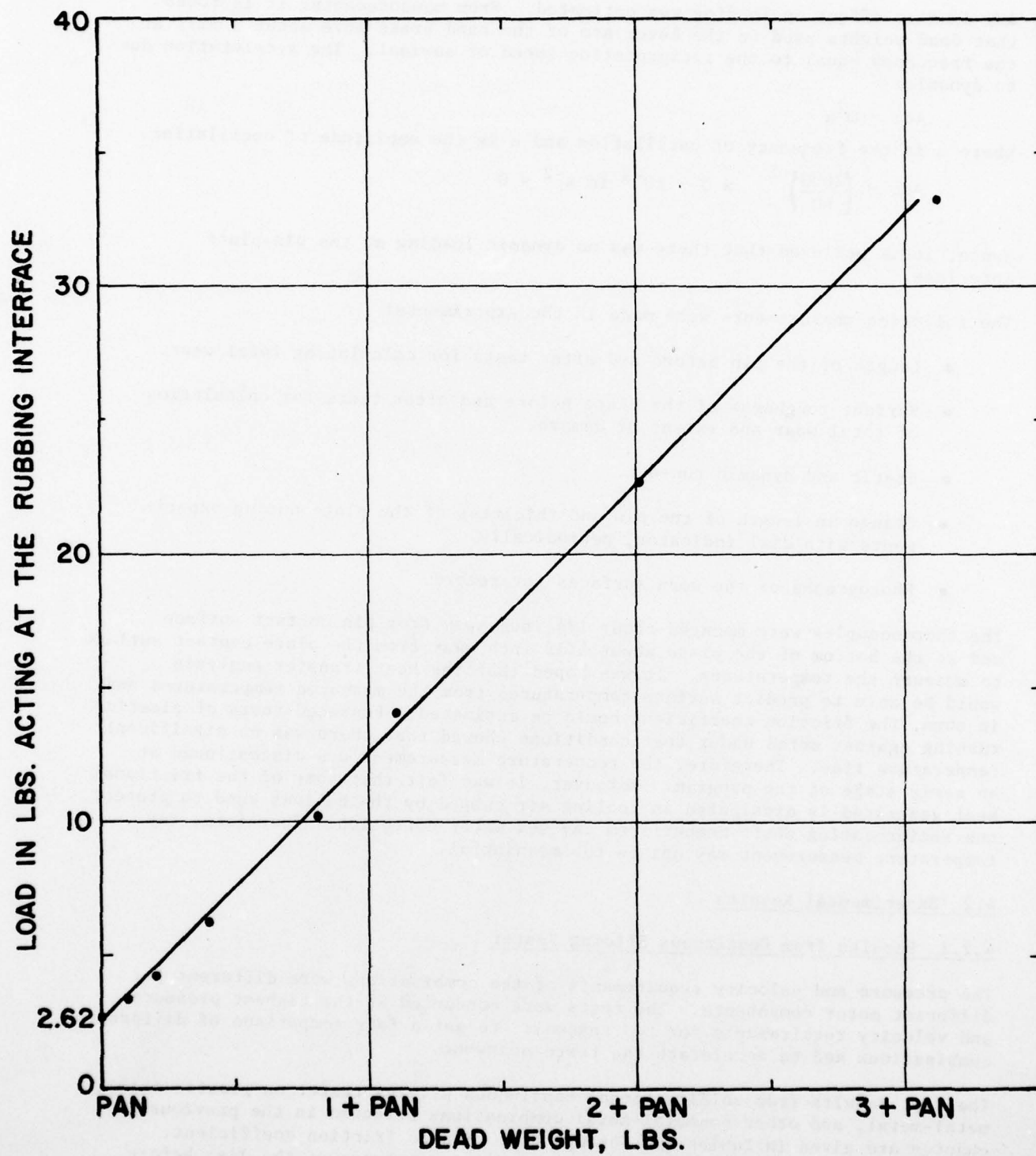
Figure 4.12 Load Calibration Curve for Reciprocating Tester

Any dynamic effect on loading was estimated. From measurements, it is found that dead weights used on the lever arm of the hand press move about 5 mils at the frequency equal to the reciprocating speed of sawzaal. The acceleration due to dynamics

$$Acc = \omega^2 a$$

where ω is the frequency of oscillation and a is the amplitude of oscillation.

$$Acc = \left(\frac{2000}{60}\right)^2 \times 5 \times 10^{-3} \text{ in s}^{-2} \simeq 0$$

Hence, it is believed that there was no dynamic loading at the pin-plate interface.

The following measurements were made in the experiments:

- Length of the pin before and after tests for calculating total wear.

- Surface roughness of the plate before and after tests for calculation of total wear and extent of damage.

- Static and dynamic run-out.

- Change in length of the pin and thickness of the plate during experiments with dial indicator, periodically.
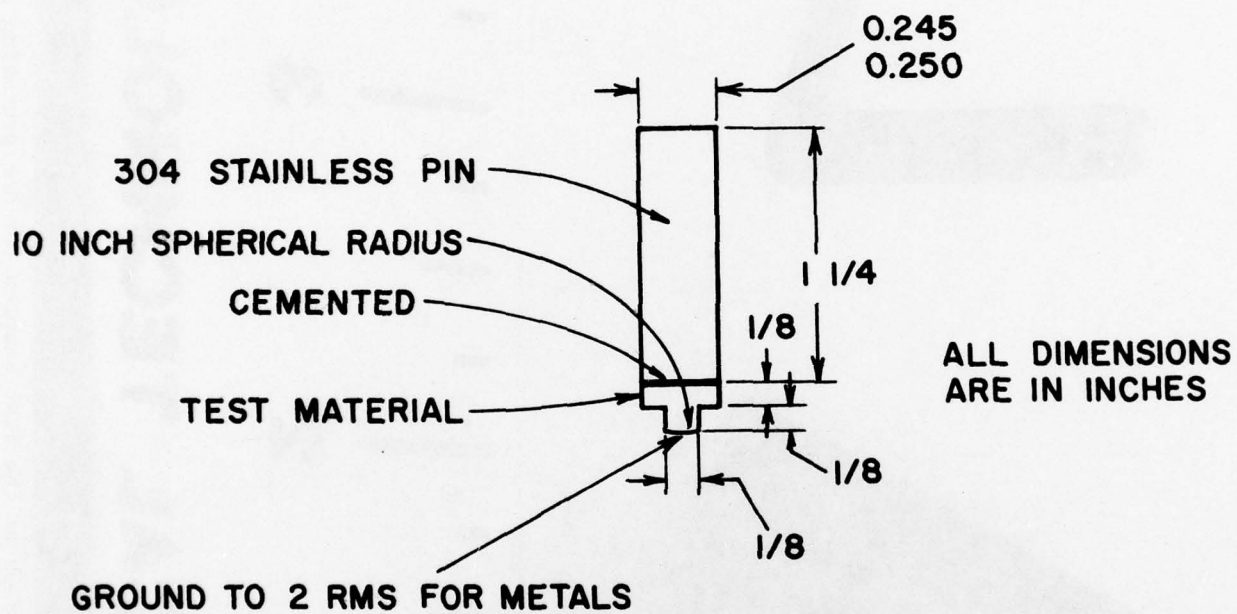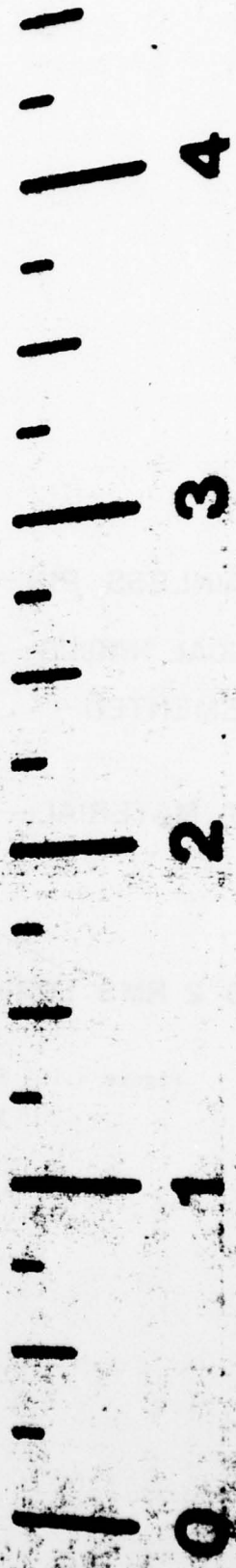
- Photographs of the worn surfaces for record.

The thermocouples were mounted about 1/4 inch away from pin contact surface and at the bottom of the plate about 1/16 inch away from the plate contact surface to measure the temperatures. It was hoped that the heat transfer analysis would be able to predict surface temperatures from the measured temperatures and, in turn, the friction coefficient could be estimated. Repeated tests of plastics rubbing against metal under test conditions showed that there was no significant temperature rise. Therefore, the temperature measurement was discontinued at an early stage of the program. Moreover, it was felt that some of the frictional heat generated is dissipated in cooling air pumped by the bellows used to protect the reciprocating shaft member from any sea water corrosion. Therefore, any temperature measurement may not be too meaningful.

4.2 Experimental Results

4.2.1 Results from Continuous Sliding Tester

The pressure and velocity requirements of the combinations were different for different motor components. The tests were conducted at the highest pressure and velocity requirements for two reasons: to get a fair comparison of different combinations and to accelerate the tests somewhat.

The test results from unidirectional continuous sliding tester on plastic-metal, metal-metal, and other nonmetal-metal combinations selected in the previous chapter are given in Tables 4.1 through 4.3. Static friction coefficient, kinetic friction coefficient, wear rate, surface roughness of the disc before and after tests, final stress, surface speed, and comments on the surface appearance of the specimens after test are included in these tables.

TABLE 4.1

ACCELERATED FRICTION AND WEAR TEST RESULTS FROM UNIDIRECTIONAL CONTINUOUS SLIDING TESTER

Plastic-Metal Combinations; Lubricant: Synthetic Sea Water

Sliding Speed = 1500 ft/min (2900 rpm); Test Duration ≈ 30 Hours Each; Temperature = Ambient (76°F)

Item No.	Test Materials		Static Friction Coeff.		Kinetic Friction Coefficient		Total Wear Rate 10^{-3} in/100 Hours	Surface Roughness of disc, μ in. (transverse)		Final Stress psi	Comments
	Pin	Disc	At Start	At Stop	Start of Test	End of Test		Before	After		
1	Torlon 4301 (Polyamide-imide with fillers)	Nitronic 50 (R_c 30)	0.22	0.275	0.014	0.009	2.7	1.2	2.5	1190	Smooth running. Fine marks on disc
2	Noryl GFN-3 30% glass filled	Nitronic 50	0.39	0.38	0.022	0.013	3.8	1.0	2.5	1065	Smooth running. Some wear of disc.
3	Polyimide, 30% PTFE Meldin PI30X	Nitronic 50	0.23	0.22	0.015	0.018	6.7	0.6	0.9	900	Smooth running. Very fine marks on disc. looks smooth.
4	DU Bearing Material	Nitronic 50	0.176	0.122	0.018	0.012	7.3	1.6	4.0	1190	Smooth running. Disc very smooth, has one groove.
5	Ultra-High molecular weight Polyethylene Cadco HMW 1900	Nitronic 50	0.092	0.034	0.022	0.02	8.3	1.5	2.0	970	Smooth running. Disc practically not worn.

NOTE: Disc wear << 0.0001 in. on diameter during any test.

ACCELERATED FRICTION AND WEAR TEST RESULTS FROM UNIDIRECTIONAL CONTINUOUS SLIDING TESTER

Plastic-Metal Combinations; Lubricant: Synthetic Sea Water

Sliding Speed = 1500 ft/min (2900 rpm); Test Duration ≈ 30 Hours Each; Temperature ≈ Ambient (76°F)

Item No.	Test Materials		Static Friction Coeff.		Kinetic Friction Coefficient		Total Wear Rate 10^{-3} in/100 Hours	Surface Roughness of disc, μ in. (transverse)		Final Stress psi	Comments
	Pin	Disc	At Start	At Stop	Start of Test	End of Test		Before	After		
6	Ultra-High molecular weight Polyethylene, 50% bronze powder filled	Nitronic 50	0.049	0.029	0.021	0.015	7.8	1.8	2.2	1120	Some stick slip. Disc has practically no wear. Pin finely scored.
7	Torlon 4301	Inco 625 (Rc24)	0.23	0.25	0.018	0.025	2.1	3.5	3.5	2180	Smooth running No marks on disc. Pin has very fine and smooth wear track.
8	Noryl GFN-3	Inco 625	0.38	0.41	0.017	0.016	3.8	2	5	1900	Disc has very fine wear marks. Pin smooth, has metallic particles embedded.
9	PT30X	Inco 625	0.18	0.26	0.013	0.012	5.9	2	4	1300	Disc practically untouched Pin has very fine marks in the central region.

TABLE 4.1
(Cont'd)
ACCELERATED FRICTION AND WEAR TEST RESULTS FROM UNIDIRECTIONAL CONTINUOUS SLIDING TESTER

Plastic-Metal Combinations; Lubricant: Synthetic Sea Water

Sliding Speed = 1500 ft/min (2900 rpm); Test Duration ≈ 30 Hours Each; Temperature = Ambient (76°F)

Item No.	Test Materials		Static Friction Coeff.		Kinetic Friction Coefficient		Total Wear Rate 10^{-3} in/100 Hours	Surface Roughness of disc, μ in. (transverse)		Final Stress psi	Comments
	Pin	Disc	At Start	At Stop	Start of Test	End of Test		Before	After		
10	Torlon 4301	MP35N (R_c 42)	0.24	0.26	0.018	0.017	3.5	2.5	4.5	1440	Smooth running. Disc and pin have very fine wear marks.
11	PI30X	MP35N	0.25	0.275	0.02	0.015	1.9	2.2	4	1190	Smooth running. Disc and pin have very fine wear tracks.
12*	Torlon 4301	Inco 625	0.2	0.23	0.023	0.016	0.5	1.4	1.6	1500	Endurance test-smooth running. Disc has only one very fine wear mark. Pin smooth and has two wear marks.
13**	Torlon 4301	Inco 625	0.25	0.25	0.012	0.010	8	3.5	4.5	1240	Smooth running. No mark on disc. Pin has smooth wear track.

* Test duration = 145 hours.

** Temperature of sea water bath – 190°F; Test duration = 7 hours.

TABLE 4.1
(Cont'd.)

ACCELERATED FRICTION AND WEAR TEST RESULTS FROM UNIDIRECTIONAL
CONTINUOUS SLIDING TESTER

Plastic-Metal Combinations; Lubricant: Synthetic Sea Water

Sliding Speed = 1500 ft/min (2900 rpm); Test Duration ≈ 30 Hours Each; Temperature = Ambient (76°F)

Item No.	Test Materials		Static Friction Coeff.		Kinetic Friction Coefficient		Total Wear Rate 10^{-3} in/100 Hours	Surface Roughness of disc, μ in. (transverse)		Final Stress psi	Comments
	Pin	Disc	At Start	At Stop	Start of Test	End of Test		Before	After		
14***	Torlon 4301	Inco 625	0.26	0.30	0.018	0.016	1.7	3.9	4.0	1900	Smooth running. No mark on disc. Pin has smooth wear track.

*** Diameter of the pin = 1/8". All others = 1/4".

4-20

TABLE 4.2

ACCELERATED FRICTION AND WEAR TEST RESULTS FROM UNIDIRECTIONAL CONTINUOUS SLIDING TESTER

Metal-Metal Combinations

Lubricant: Synthetic Sea Water, Temperature = Ambient (76°F)

Item No.	Test Materials Pin	Test Materials Disc	Static Friction Coeff. At Start	Static Friction Coeff. At Stop	Kinetic Friction Coeff. Start of Test	Kinetic Friction Coeff. End of Test	Total Wear Rate in/100 Hours	Surface Roughness of disc, μ in. (transverse) Before	Surface Roughness of disc, μ in. (transverse) After	Instantaneous Hertzian Stress, psi	Final Hertzian Stress, psi	Sliding Speed fpm	Test Duration, hours	Comments
1+	Leaded tin bronze SAE 660	440C heat treated (R_C55)	0.13		Almost zero	Almost zero	Very Little	1.4		4600	≈200	775	.25	Very smooth running
					0.05 to 0.2	0.05 to 0.2	0.5		1.4		720	1500	.35	Violent stick slip, noisy. Disc is untouched. Pin has smooth wear tracks.
2	Waukesha 88 (R_B77)	MP35N (R_C42)			0.12			3		5400		775	.25	Noisy, some stick slip.
						0.36	4.7		14		300	775	.25	Noisy, stick slip, local welding & scoring on pin and disc. Disc slightly discolored.
3	Nitronic 50 (R_C30)	MP35N (R_C42)	0.54	0.54	.06 to 0.5	Very high	1.8	2	36	5200	35	775	.10	Very noisy, violent stick slip
												1500	.33	Very noisy, violent stick slip. Water and disc turned black. Pronounced welding and scoring on pin and disc.

TABLE 4.2 (Cont'd.)

ACCELERATED FRICTION AND WEAR TEST RESULTS FROM UNIDIRECTIONAL CONTINUOUS SLIDING TESTER

Metal-Metal Combinations

Lubricant: Synthetic Sea Water, Temperature = Ambient (76°F)

Item No.	Test Materials		Static Friction Coeff.		Kinetic Friction Coeff.		Total Wear Rate in./100 Hours	Surface Roughness of disc, μ in. (transverse)		Instantaneous Hertzian Stress, psi	Final Stress, psi	Sliding Speed, fpm	Test Duration, hours	Comments
	Pin	Disc	At Start	At Stop	Start of Test	End of Test		Before	After					
4	440C (R_c55)	440C (R_c55)	0.65	0.68	0.5	0.03	0.05	2	13	5400	86	775	1	Initially running rough stick slip, local welding and scoring of pin and disc.
5*	Waukesha 88 (R_B77)	MP35N (R_c42)	0.32	0.14	0.28	0.025	2.8	1.6	13	5400	29	775	0.5	Some stick slip. Pronounced welding and scoring on pin and disc.
6**	Nitronic 50	MP35N	0.42	0.34	Very high	Very high	6.0	1.6	28	5200	40	775	0.1	Violent stick slip. Pronounced scoring on pin and disc.
7***	Nitronic 60 (R_c22)	MP35N (R_c42)	0.41	0.36	0.22	0.05	0.028	8	19	5400	50	1500	4	Initially running rough, stick slip. Scoring of pin and disc.

* The test was conducted with 50 μg/g Polyox coagulant additive in the sea water.
** The test was conducted with 500 μg/g Polyox coagulant additive in the sea water.
*** Surfaces of pin and disc before test were rougher than previous experiments.

TABLE 4.2 (Cont'd.)

ACCELERATED FRICTION AND WEAR TEST RESULTS FROM UNIDIRECTIONAL CONTINUOUS SLIDING TESTER

Metal-Metal Combinations

Lubricant: Synthetic Sea Water, Temperature = Ambient (76°F)

Item No.	Test Materials		Static Friction Coeff.		Kinetic Friction Coeff.		Total Wear Rate in./100 Hours	Surface Roughness of disc, μ in. (transverse)		Instantaneous Hertzian Stress, psi	Final Stress, psi	Sliding Speed fpm	Duration, hours	Comments
	Pin	Disc	At Start	At Stop	Start of Test	End of Test		Before	After					
8***	440C (R_c 55)	440C (R_c 55)	0.53	0.53	0.32	0.03	0.012	11	13	5400	65	1500	4	Initially running rough, stick slip. Scoring of pin and disc.

*** Surfaces of pin and disc before test were rougher than previous experiments.

+ Diameter of pin - 1/4 inch, all others 1/8".